

MICROSCALE HYDRODYNAMIC CAVITATION
AND ITS BIOMEDICAL APPLICATIONS

OSMAN YAVUZ PERK

Submitted to the Graduate School of Engineering and Natural Sciences
in partial fulfillment of
the requirements for the degree of
Master of Science

SABANCI UNIVERSITY

MICROSCALE HYDRODYNAMIC CAVITATION
AND ITS BIOMEDICAL APPLICATIONS

APPROVED BY:

Dr. Ali Koşar

(Thesis Supervisor)

Dr. Devrim Gözüaçık

Dr. Işın Ekici

Dr. Alpay Taralp

Prof. Dr. Ali Rana Atılğan

DATE OF APPROVAL: 07/08/2012

© OSMAN YAVUZ PERK 2012

ALL RIGHTS RESERVED

MICROSCALE HYDRODYNAMIC CAVITATION
AND ITS BIOMEDICAL APPLICATIONS

Osman Yavuz Perk

Mechatronics Engineering, M.Sc. Thesis, 2012

Thesis Supervisor: Dr. Ali KOŞAR

Keywords: Hydrodynamic cavitation, biomedical treatment, microchannel, cavitation
damage, kidney stone erosion

ABSTRACT

Micro flows find applications in a variety of topics covering biomedical, cooling, electronics and MEMS (micro-electro-mechanical-systems) applications. Hydrodynamic cavitation, which is one of the types of cavitation, is based on vaporization, bubble formation and bubbles implosion at low pressures. When the local static pressure of the liquid drops below the vapor pressure of the medium at the operating temperature, cavitating flow is generated. The collapses of the cavities give rise to serious damage to the exposed surfaces. Catastrophic damage and destructive nature of hydrodynamic cavitation has been preferred to be used in various biotechnological areas, but yet not for biomedical purposes. Therefore, in this study, it is focused on its effect on biological samples to determine its feasibility and controllability for biomedical usage.

The objective of this study is to reveal the potential of micro scale hydrodynamic bubbly cavitation for the use of kidney stone treatment, and to reveal the effects on prostate cells and benign prostatic hyperplasia (BPH) tissue. Hydrodynamically generated cavitating bubbles were targeted to the surfaces of 18 kidney stone samples made of calcium oxalate, and their destructive effects were exploited in order to remove kidney stones in *in vitro* experiments. Phosphate buffered saline (PBS) solution was used as the working fluid under bubbly cavitating conditions in a 0.75 cm long micro probe of 147 μm inner diameter at 9790 kPa pressure. The surface of calcium oxalate type kidney stones were exposed to bubbly cavitation at room temperature for 5 to 30 min. The eroded kidney stones were visually analyzed with a high speed CCD camera and using SEM (scanning electron microscopy) techniques. The results showed that at a cavitation number of 0.017, hydrodynamic bubbly cavitation device could successfully erode stones with an erosion rate of 0.31mg/min. It was also observed that the targeted application of the erosion with micro scale hydrodynamic cavitation may even cause the fracture of the kidney stones within a short time of 30 min. The proposed treatment method has proven to be an efficient instrument for destroying kidney stones.

In cell culture experiments, hydrodynamic cavitation caused a dramatic decrease in cell number. Moreover, late response of hydrodynamic cavitation was checked with various cell death assays. However, no effect was observed in terms of cell death activation. In addition to prostate cells, the destructive effect of hydrodynamic

cavitation was investigated on human tissues. Hydrodynamic cavitation exposure resulted in a deep cavity on the targeted area of BPH tissue without giving any damage to the surrounding area. All these new findings support the idea of usage of hydrodynamic cavitation as a novel therapeutic method for ablating tumor tissues.

MİKRO ÖLÇEKTE HİDRODİNAMİK KAVİTASYON
VE BİYOMEDİKAL UYGULAMALARI

Osman Yavuz Perk

Mekatronik Mühendisliği, Yüksek Lisans Tezi, 2012

Tez Danışmanı: Dr. Ali KOŞAR

Anahtar Kelimeler: Hidrodinamik kavitasyon, biomedical tedavi, mikrokanal, böbrek
taşı erozyonu

ÖZET

Mikro akışkanların biyomedikal, soğutma, elektronik ve MEMS (mikro-elektromekanik-sistemler) gibi bir çok alanda uygulamaları bulunmaktadır. Kavitasyon çeşitlerinden biri olan "hidrodinamik kavitasyon" temel olarak düşük basınçlarda buharlaşma, baloncuk oluşması ve baloncuk patlamasıdır. Sıvının lokal statik basıncı sıvının o sıcaklıktaki buhar basıncının altına düştüğünde kavitesyon akışı elde edilmiş olur. Bu baloncukların yüzeylere uygulanması yüzeylere çok ciddi zarar verir. Kavitasyonun yıkıcı ve katastrofik doğası bir çok biyoteknolojik alanda kullanılmasına rağmen biyomedikal amaçla kullanılmamıştır. Bu yüzden bu çalışma kavitasyonun biyolojik örnekler üstüne etkisi, uygulanabilirliği ve kontrol edilebilirliği üzerine yoğunlaşmıştır. Bu çalışmada mikro ölçekte hidrodinamik baloncuklu kavitasyonun böbrek taşı hastalığı tedavisinde kullanımı, prostat hücreleri ve benign prostatic hyperplasia (BPH) dokusu üstündeki etkisini görme konularına yoğunlaşmıştır. Hidrodinamik olarak oluşturulmuş kavitasyon baloncukları 18 tane kalsiyum oksalat böbrek taşı üstüne uygulanmış ve yıkıcı etkileri in vitro deneyler ile ölçülmüştür. Çalışma sıvısı olarak Phosphate buffered saline (PBS) solüsyonu baloncuklu kavitasyon şartlarında ve 0.75 cm uzunluğunda, 147 µm iç çapında mikro prob ile 9790 kPa basıncında kullanılmıştır. Böbrek taşlarının yüzeyleri oda sıcaklığında 5 dakikadan 30 dakikaya kadar baloncuklu kavitasyona maruz bırakılmıştır. Erozyona uğramış böbrek taşları görsel olarak yüksek hızlı CCD kamera ve SEM (scanning electron microscopy) kullanarak incelenmiştir. Sonuçlar şunu gösteriyor ki 0.017 kavitasyon sayısı ile hidrodinamik kavitasyon düzeneği böbrek taşlarını 0.31mg/min erozyon hızı ile başarılı bir şekilde eritmektedir. Ayrıca uygulanan hidrodinamik kavitasyonun 30 dakika gibi kısa bir sürede böbrek taşlarının kırılmasına da yol açabildiği gözlemlenmiştir. Önerilen metodun böbrek taşlarının tedavisi konusunda etkili bir araç olabileceği kanıtlanmıştır. Hücre kültürü deneylerinde hidrodinamik kavitasyon hücre sayısında dramatik bir düşüşe sebep olmuştur. Ayrıca, hidrodinamik kavitasyona sonraki tepki de kontrol edilmiş, ve hücre ölümü aktivasyonu bakımından herhangi bir bir etki gözlemlenmemiştir. Prostat hücrelerine ek olarak hidrodinamik kavitasyonun insan dokusu üstündeki yıkıcı etkisi de incelenmiştir. Hidrodinamik kavitasyon BPH dokusu üstündeki hedeflenen alanda diğer alanlara herhangi bir hasar vermeden derin bir oyuk oluşturmuştur. Tüm bu bulgular hidrodinamik kavitasyonun tümör dokularının sökülmesi için özgün bir terapötik metod olduğunu desteklemektedir.

ACKNOWLEDGEMENTS

First and foremost I wish to thank my thesis supervisor DR. Ali KOŞAR. He has been supportive since the days when I was an undergraduate. Ever since he has supported me not only financially but also academically and emotionally through the rough road to finish this thesis.

I also would like to thank to my homie, my honorary brother Türker İzci for his endless friendship and support. We have started and finished mechatronics master together. I owe him very much.

I'd like to present my special thanks to my padawan, my source of happiness Ebru Demir, without her compassion and sympathy, it would have been impossible for me to handle these rough times (may the force be with her).

I am very thankful to my family for the constant psychological support that they have provided. Without anacığım and babacığım and my little brother I would not be who I am today.

I send my sincere thanks to my colleagues Muhsincan Şeşen and Zeynep İtah, with whom I have done countless cavitation experiments at early morning hours, for their patience, motivation, enthusiasm and immense knowledge.

I am also grateful to my thesis committee members Dr. Devrim Gözüaçık, Dr. Işın Ekici, Dr. Ali Rana Atılğan and Dr. Alpay Taralp for giving their valuable time commenting on my thesis and their valuable ideas during my study in this university.

This work was supported by Sabancı University Internal Grant for Research Program under Grant IACF09-00642.

TABLE OF CONTENTS

ABSTRACT.....	v
ÖZET	viii
TABLE OF CONTENTS.....	x
LIST OF FIGURES	xi
LIST OF TABLES	xiii
NOMENCLATURE	xiv
1 INTRODUCTION	1
1.1 Micro Scale Hydrodynamic Cavitation.....	1
1.1.1 Overview on Cavitation Inception.....	1
1.1.2 Micro vs. Macro Scale Cavitation	5
1.1.3 Cavitation on Kidney Stones	6
1.1.4 Cavitation on prostate cells and tissues	7
2 EXPERIMENTAL.....	11
2.1 Experimental Setup and Procedure for Hydrodynamic Cavitation.....	11
2.1.1 Materials and Methods	11
2.1.2 Calcium Oxalate Real Kidney Stone Samples as a Model.....	13
2.2 Experimental Procedure for Prostate cells and Tissue	16
2.2.1 Cell line, cell culture and treatments	16
2.2.2 Experimental set-up and procedure	17
2.2.3 Cavitation Pressure Kinetics and Exposure Time Kinetics Experiments.....	17
2.2.4 Cell counting and Cell Death Analysis of Cavitated Samples	18
2.2.5 Cell Cycle Analysis	18
2.2.6 DNA Fragmentation Assay	18
2.2.7 Cavitation Experiments on Human Benign Prostatic Hyperplasia (BPH) Tissue 19	
2.2.8 Hematoxylin and Eosin Staining	19
2.2.9 Statistical Analysis	19
3 RESULTS AND DISCUSSION.....	20
3.1 Results and Discussion of Hydrodynamic Cavitation Study	20
3.1.1 Results and Discussion of Kidney Stone Experiments.....	20
3.1.2 Results and Discussion of Prostate Cells and Tissue Experiments	27
4 CONCLUSION.....	36
4.1 Conclusion of Hydrodynamic Cavitation Study	36
4.1.1 Conclusion of Hydrodynamic Cavitation Application to Chalk and Cancerous Cells.....	36
4.1.2 Conclusion of Hydrodynamic Cavitation Application to Prostate Cells and Tissue 40	
References.....	42

LIST OF FIGURES

Figure 1 Cavitation damage on a valve plate for an axial piston hydraulic pump.	1
Figure 2 Cavitation in flow through orifice and the Hydraulic Gradient Line (HGL) .	3
Figure 3 Erosion by hydrodynamic bubbly cavitation.....	4
Figure 4 Microchannel configuration with the orifice throat and exit area	11
Figure 5 Experimental setup	12
Figure 6 Visible cavitation cloud for the specified experimental setup incepts at inlet pressures between 50-70psi	14
Figure 7 Experimental placement of the kidney stone.	14
Figure 8 Volumetric flow rates as a function of inlet pressure. (Cavitation is observed over the entire range of pressure)	20
Figure 9 Cavitation bubble cloud images captured by the high speed camera. (1) Inlet. (2) Micro probe (Orifice throat) (3) Bubble Cloud.	21
Figure 10 Kidney stone before exposure to bubbly cavitation. (b) Erosion on kidney stone after exposure to bubbly cavitation.	22
Figure 11 (a), (b) and (c). Experimental results of kidney stone as a function of time (min). Broken stones are marked with black circle.	23
Figure 12 Stone debris	24
Figure 13 (a) Average erosion amount (g) vs. time (min) graph at 9790 kPa pressure, 1mm probe gap. Bubbly cavitation sets are at the top. Control experiments are at the bottom. (b) Average erosion amount (in %) vs. time graph at 9790 kPa pressure, 1mm probe gap.....	25
Figure 14 (a) Stabilized sample (b) Free rotating sample in 5cc container	26
Figure 15 (a) Erosion in bubble path direction for stationary sample (b) Erosion in every direction for rotating sample	26
Figure 16 Average erosion amount for stationary samples (in %) and erosion amount for stationary samples (in %) vs. time graph at 9790 kPa pressure	27
Figure 17 Hydrodynamic cavitation caused a dramatic decrease in cell number in a exposure time dependent manner. Hydrodynamic cavitation exposed on prostate cancer cells; PC-3 and DU-145 under an inlet pressure of 150 PSI for 1, 2, 3 and 5 minutes. Control samples were unexposed to cavitation. Cell death ratio of A) PC-3 and B) DU-145 and cell numbers of C) PC-3 and D) DU-145 were determined after cavitation (0 h) and 24 hours later. Cell death was analyzed via trypan blue exclusion assay and cell numbers of each sample were normalized to values of control sample at 0 h. Data are shown as mean \pm S.D (n=3, Student t-test * p<0.05, ** p<0.01, *** p<0.001).....	29
Figure 18 Apoptotic activity was not induced following to hydrodynamic cavitation exposure on prostate cells. No PARP cleavage and caspases activation was checked after cavitation. Hydrodynamic cavitation effect on prostate cancer cells; PC-3 and DU-145 A) with a pressure kinetics (50, 100 and 150 PSI) at a constant exposure time (5 min) was checked by means of apoptotic activity at 0 h (immediately after cavitation) and 24 hours after cavitation. Control samples were unexposed to cavitation. 8 μ M Staurosporine and 10 μ M Cisplatin treated samples are used as positive control for apoptosis activation.....	31
Figure 19 Hydrodynamic cavitation did not induce autophagy. Autophagic activity was checked with p62 degradation and LC3-I to II shifting. Hydrodynamic cavitation impact on prostate cancer cells; PC-3 and DU-145 with a pressure kinetics (50, 100 and 150	

PSI) at a constant exposure time (5min) was controled by means of autophagy at 0 h (immediately after cavitation) and 24 hours after cavitation. Control samples were unexposed to cavitation. 8 μ M Staurosporine and 10 μ M Cisplatin treated samples are used as positive controls.	32
Figure 20 The reduction of cell growth following to hydrodynamic cavitation was not caused by neither cell cycle arrest nor DNA fragmentation. PC-3 cells were exposed to 150 PSI, 5 min cavitation and cultured for 0, 6, 12 and 24 hours. Control samples were unexposed to cavitation. A) There was no difference in cell cycle of cavitation exposed cells in comparison to cavitation unexposed cells. Cell cycle arrest analysis of PC-3 was performed by flow cytometry at 0, 6, 12 and 24 hours after cavitation. Etoposide, positive control, treatment caused cells arrest in M phase. Data are shown as mean \pm S.D (n=3). B) Hydrodynamic cavitation did not cause any DNA breaks leads to DNA fragmentation. Cavitation samples did not have any fragmentized DNA as well as cavitation unexposed control samples. C)	33
Figure 21 Hydrodynamic cavitation eroded the human BPH tissue effectively and precisely. A) Cavitation control (at same flow rate, yet different pressure with cavitation) and cavitation (1450 PSI) exposed BPH tissues for 15 and 30 minutes were observed under 40X. Histopathological analysis was done with H&E staining.	35
Figure 22 Calcium oxalate kidney stone (a) before hydrodynamic cavitation exposure, (b) after hydrodynamic cavitation exposure.	38
Figure 23 A typical endoscopy device.....	39
Figure 24 Crossection of cavitation probe integration for endoscope	39

LIST OF TABLES

Table 1 Material properties of calcium oxalate kidney stones. [61].....	13
Table 2 Kidney stone experiment sets. Fractured stones are marked with (*).....	15

NOMENCLATURE

P_1	Local static pressure at point 1
P_2	Local static pressure at point 2
V_1	Fluid Velocity at point 1
V_2	Fluid Velocity at point 2
P_∞	Pressure at the exit
P_v	Vapor pressure of the fluid
C_i	Cavitation number
R_{max}	Maximum bubble radius
R_p	Particle radius (average bubble radius in this study)
V_{th}	Flow Velocity
E_t	Young's modulus of elasticity
f	Friction coefficient
W	Erosion rate

Greek Symbols

ρ	Density
ν	Kinematic viscosity
σ	Cavitation number
σ_b	Flexural strenght

1 INTRODUCTION

1.1 Micro Scale Hydrodynamic Cavitation

1.1.1 Overview on Cavitation Inception

Hydrodynamic cavitation is the formation of gas bubbles in a liquid region due to a sudden pressure drop of the liquid below its vapor pressure. This pressure drop leads to vaporization and bubble generation even at room temperatures. When successfully targeted on desired surfaces, the cavitation bubbles collapse upon subjection to atmospheric pressure. This process leads to the emergence of energetic shock waves that are highly destructive and might cause significant damage on exposed surfaces. [1]

Effects of cavitation offer a research topic for various researchers and for most of the cases, and associated with catastrophic damage, flow choking, low efficiency, acoustic noise and destruction. For this reason, destructive aspect of hydrodynamic cavitation has been caused much concern in the design of conventional scale hydraulic machinery (Figure 1).



Figure 1 Cavitation damage on a valve plate for an axial piston hydraulic pump [2].

There are two main sources for creating cavitating flow: hydrodynamic and ultrasonic

sources. The use of ultrasonic cavitation in treatment of cancerous tissues has been investigated by various researchers and has been widely employed. As a result, ultrasonic sources have been the most popular means of generating cavitation in laboratory scale studies, and numerous applications of ultrasonic cavitation (including biomedical applications). This method is a non-invasive treatment, where some difficulties are faced in targeting the precise location (kidney stone, cancerous prostate tissue) of the treatment. Hydrodynamic cavitation is another candidate with a cost effective and energy efficient solution [3] [4] [5] in biomedical treatment. With the emergence of microfluidics; hydrodynamic cavitation has been considered as an important alternative to ultrasonic cavitation over the last decade. Pioneering studies on hydrodynamic cavitation in microchannels have been successful in showing the unique properties of cavitating flow at the microscale [6] [7] [8] [9] [10].

Reduction of static pressure in a fluid to a critical value (vapor pressure) results in cavitation. As a result of this, cavitation inception by means of vapor-gas bubbles or larger scale super cavities occurs. The basic requirement for hydrodynamic cavitation is the reduction of static pressure to a critical value. Cavitating flows could be created by using a micro channel configuration with a micro orifice design at the outlet. A dramatic pressure drop in response to the sudden reduction in flow area assures cavitation.

The reduction in static pressure can be achieved an acceleration of the fluid and a consequent increase in the fluid velocity between points 1 and 2 (Figure 2, HGL 1). The critical location (point 2, Vena Contracta), where the static pressure drops to its minimum, the velocity rises to its maximum. As the fluid passes through the orifice throat, the velocity of the fluid increases due to conservation of mass. Local static pressure of the fluid decreases in consistency with the Bernoulli equation (1) (with the assumption of no frictional losses through the orifice and neglecting frictional losses through the orifice).

$$\frac{P_1}{\rho} + \frac{1}{2}V_1^2 = \frac{P_2}{\rho} + \frac{1}{2}V_2^2 \quad (1)$$

where ρ is the density of the fluid, P_1 and P_2 are local static pressures, V_1 and V_2 are fluid velocities at before the orifice and inside the orifice, respectively. The reduction in static pressure leads to an acceleration of the fluid due to the equation (1) and as a result of this, velocity of the fluid increases between points 1 and 2 (Figure 2).

Further reduction in the exit pressure reduces the static pressure at the Vena Contracta down to the vapor pressure of the liquid (HGL 3). Once this physical limit is reached, any attempt to increase the discharge by reducing the exit pressure is futile. This situation is defined as choked flow or choked cavitation where the exit pressure loses its control over the discharge. The micro-orifice produces its maximum discharge under these conditions, and any reduction in the exit pressure only results in the elongation of the vapor cavity (HGL 4, HGL 5), which is characterized as supercavitating flow.

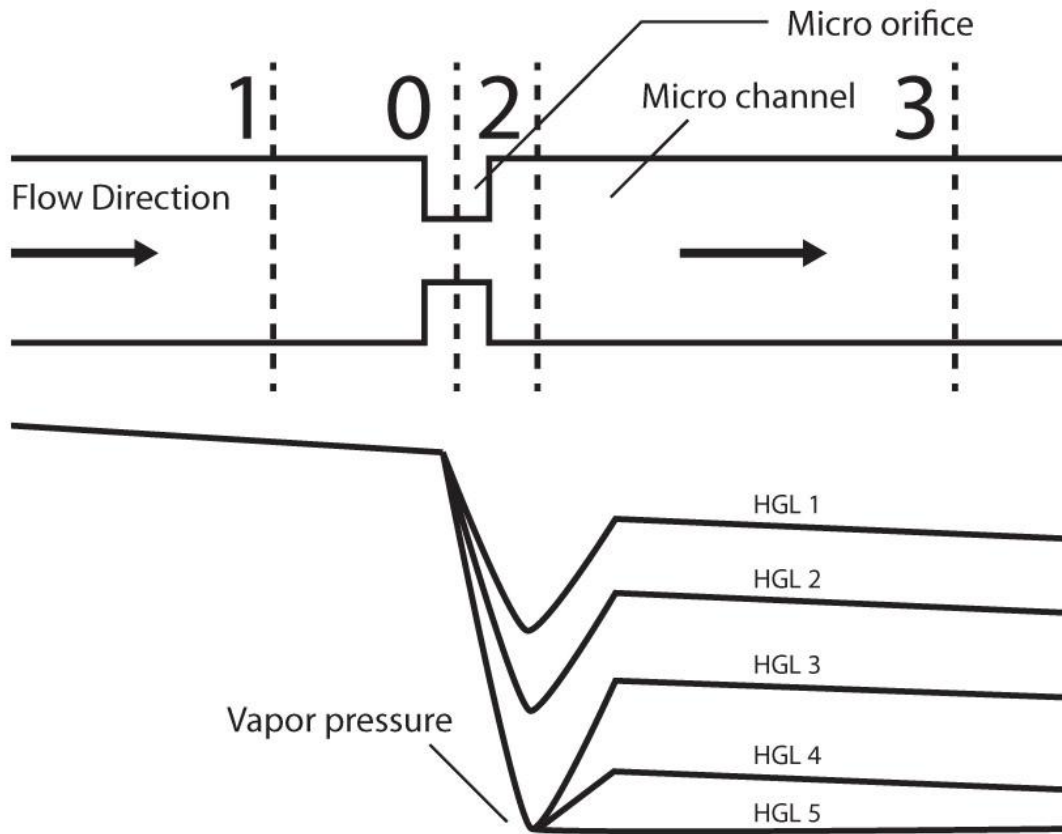


Figure 2 Cavitation in flow through orifice and the Hydraulic Gradient Line (HGL)

In order to characterize intensity of the cavitation, a dimensionless number, cavitation number C_i can be calculated as;

$$C_i = \frac{P_\infty - P_v}{\frac{1}{2}\rho V^2} \quad (2)$$

where ρ is the density, V is the flow velocity at the micro-orifice, P_v is the vapor pressure and P_∞ is the exit pressure. Geometry of the channel has a great influence on the formation of cavitation. Lower cavitation number results in more intense cavitation, while larger cavitation numbers suggest weaker cavitation and eventually non-cavitating hydrodynamic flow conditions.

Generally, cavitation is related with the explosive growth and disastrous collapse of vapour bubbles. The catastrophic implosions produce pulses of pressure in the order of 100 bar resulting damage on the applied surfaces [11] [12].

Cavitation erosion is caused by the repetitive impingement of cavitation-induced bubbles on a solid flow boundary.[1] Most of the early observations of cavitation damage were made on machines, such as ships' propellers and hydraulic turbines, which operated in a liquid medium.[13] The same damaging effects of collapsing bubbles have been exploited as a tool in kidney stone therapy, namely, surgery, and lithotripsy.[14]

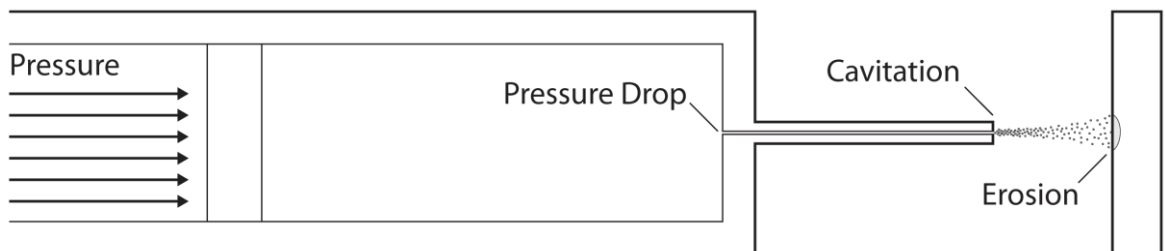


Figure 3 Erosion by hydrodynamic bubbly cavitation.

Various parameters (pulse repetition frequency (PRF), pulse duration (PD), and gas content of liquid) affect the erosion rate and energy efficiency [15]. Pulsed cavitation has been explored in a variety of biological effects in the past 20 years, e.g., lung hemorrhage, intestinal hemorrhage, bone repair, and creating cavities in the ventricular wall. Some studies show that very short pulses (10–20 μ s) can produce effective bioeffects [16] [17].

1.1.2 Micro vs. Macro Scale Cavitation

Similarities

Single-phase flow through a micro-orifice is mostly similar to those observed for large orifices. The discharge and the pressure drop in flows through a microorifice share a quadratic relationship, which has also been observed in larger orifices [9]. The discharge coefficient remains constant during single-phase flow and is independent of any Reynolds number or size scale effects. The desinent cavitation number is always higher than the incipient cavitation at any scale although, at the microscale, the difference between them is considerably large [9]. Neither velocity nor pressure effects are present in cavitation inception for either the micro- or macro-orifices [6]. The choking cavitation number is also independent of any velocity or pressure scale effects. The orifice discharge coefficient falls when flow transitions from single-phase to two-phase cavitating flow. Finally, cavitation is a destructive phenomenon and can cause damage and adversely affect the performance of both micro and macro hydraulic devices.

Deviations

A much larger effort is required to instigate cavitation at the microscale. At the microscale, cavitation is also extremely difficult to eradicate once it develops. As a result, huge differences between the desinent and incipient cavitation numbers can be observed in microscale [18] [19] [20] [21] [22]. The quick transition from incipient cavitation to choking cavitation in microorifices is in contrast to the trend observed in larger orifices. The presence of a few vapor bubbles near the Vena Contracta is sufficient to choke the flow at such small scales.

Choking of the flow rate is mostly observed after the establishment of a stationary cavity a few downstream of the micro-orifice [18] [19] [20] [21] [22], which has not been reported in any previous investigation on larger orifices. The choking cavitation number does not match the predicted results unlike the results obtained for larger scales.

The small stream nuclei residence time coupled with the ability of the liquid to withstand low pressures without rupturing delays the formation of the stationary cavity

and results in lower inception cavitation number in micro scale. In macro-scale studies, the cavitation number has to be sufficiently lowered beyond choking conditions for supercavitation to develop. In larger orifices, a vapor cavity can be observed encompassing a thick liquid jet, which breaks up after hitting the walls of the pipe downstream of the orifice. Hence, the supercavitating flow pattern in micro-orifices is radically different from those on larger orifices. Once the cavitation bubbles are formed, they modify the flow rate since the bubble size is comparable with the micro-orifice or the microchannel dimension. Much lower flow rates can be observed at the same pressure difference and a significant flow hysteresis is present. The large flow hysteresis causes the exit pressure to lose control over the discharge. This has never been a concern for designers of conventional scale hydraulic machinery.

Surface nuclei, which are less dominant than the stream nuclei at macro-scale, are expected to have considerable influence on cavitation at the microscale [18] [19] [20] [21] [22]. The materials used in MEMS/ Microfluidic devices and specimens are different from those used in fabricating hydraulic machinery in the macro world. As a result, damage characteristics in micro devices will certainly be different and deserves a comprehensive investigation.

1.1.3 Cavitation on Kidney Stones

Kidney stone disease is a very common health problem. Approximately 5% of women and 10% of men suffer from kidney stone formation at least once in their lives. Urinary stones may be the result of genetic predisposition, due to some abnormalities of kidney anatomy (e.g. horseshoe kidney), chronic and/or metabolic abnormalities (e.g. renal tubular acidosis), medication, diet-related or secondary infections. They might be the cause of discomfort, pain, and bleeding and lead to serious complications such as kidney dysfunction or difficult to cure infections. For that reason, most of the stones need to be removed. In addition to drug treatment and dietary restrictions, the common treatment for stone disease is open surgery, retrograde or percutaneous antegrade endoscopic surgery or shock wave lithotripsy. The latter is a popular approach to treat kidney stones in selected cases, by their destruction into small pieces using sound waves, so that they can more easily pass into the bladder and eventually discarded or extracted. However, the procedure is associated with pain or discomfort. [23] [24] For this reason, light anesthesia or sedation are required to minimize these effects and

increase the patient's comfort. As other side effects, the patient might experience blood in the urine, internal bleeding, pain as the smaller stone particles pass through the ureters and urethra and skin bruising, particularly on the back or abdomen. [23] [24] Moreover, the technique may be commonly implemented only for stones located in the kidney and for those less than 1 to 2 centimeters in size. Repetitive or multi-session applications of this technique are necessary for larger or multiple stones.

Depending on the etiology, chemical composition of stones is various. A majority of kidney stones are calcium based ones, with calcium oxalate (CaOx) and calcium phosphate (CaP) accounting for approximately 80% of all of those stones, while uric acid (UA) accounts for approximately 9%, and struvite (magnesium ammonium phosphate hexahydrate) has a percentage of 10%. [25] Calcium-based stones including calcium Oxalate (CaOx) stones are especially hard and their physico-chemical properties impose a greater difficulty for the application of shock wave lithotripsy [26], which is generally suitable for softer stones such as uric acid stones.

Kidney stones are common health problems and a significant share of health expenses in any year is spent in their treatment. Therefore, novel, cost effective and innovative methods of treatment should be explored. We have previously introduced the potential of hydrodynamic cavitation for the use in biomedical therapy, and evaluated its destructive effects on cancer cells. [27] In the same study, original experiments were conducted on chalk as a model of kidney stones. Effective erosion on the specimen's surface in this study has proven the future implementation of the method on natural kidney stones from patients. As an extension of our previous work, here we explored the effect of hydrodynamic cavitation on CaOx based kidney stones obtained from 18 patients. We assessed the capability and applicability of the hydrodynamic cavitation method for kidney stone treatment and compared the proposed therapeutic application to the existing methods (e.g. ultrasound treatment). Our study introduces for the first time hydrodynamic cavitation as an alternative and effective kidney stone destruction method.

1.1.4 Cavitation on prostate cells and tissues

Cavitation is based on sequential events; the generation, growth and violent collapse of microscopic vapor bubbles in the liquid. The oscillations of bubbles produce

mechanical forces like shear forces [28] [29]. Moreover, the collapse of bubbles release strong burst energy results in great rise of the temperature (to about 10^4 K) and pressure (to about 10^4 bar) without changing the overall environmental conditions [30]. In addition to its physical effects, the implosion of the bubbles causes hemolytic cleavage of molecules, thus generates reactive oxygen species (ROS) in the liquid which gives damages to applied samples chemically [31]. All these outcomes of implosion of cavitation bubbles give damage to applied biological samples such as cells [32] [33] [34] [35] [36] and tissues. Cavitation can be generated by two main sources; ultrasound and hydrodynamic. Ultrasound cavitation is formed by applying frequency (16 kHz-100 MHz) of sound waves onto the liquid media while hydrodynamic cavitation generates bubbles by subjecting the liquid velocity fluctuations by creating constrictions in the liquid flow.

Hydrodynamic cavitation occurs when the local pressure declines below its critical point, which is the saturated vapor pressure of the liquid at the application temperature. Its destructive effect has been used for biotechnological purposes such as microbial cell disruption [37] [38], sterilization of waste waters [39] [40] and fluids [41] [42], biodiesel production [43] and nano-particles generation [44]. The rapid emergence of cavitation applications *in vivo* gives rise to question the possibility and feasibility of the usage of hydrodynamic cavitation for therapeutic approaches.

Biological effects of ultrasound cavitation are known in a more detailed way and its therapeutic use against cancerous tissues has been investigated with both *in vitro* and *in vivo* studies. Low intensity ultrasound cavitation can enhance drug uptake, drug delivery and gene transfers into cells (less than 100 kHz) via transient disruption of cell membrane [45]. Hence, it can provide combinatory therapy to conventional methods against diseases like cancer. Furthermore, high frequency ultrasound cavitation causes irreversible cell damage results in instant cell lysis and induction of cell death (apoptosis) in various cancer cells *in vitro*[32] [33][46] and tissue damage *in vivo* through necrosis and apoptosis [47]. Therefore, ultrasound exposure leads to tissue ablation. HIFU (high intensity focused ultrasound) is the most clinically used cavitation method for tumor tissue ablation [48] [49] against benign prostatic hyperplasia (BPH) [50], prostate [51], breast [52], liver [53], renal [54] and pancreatic tumors [55] and uterine fibroids. It is a thermal non-invasive and extracorporeal treatment methodology

that uses high-intensity focused ultrasound beams to heat and ablate pathogenic tissue rapidly. Also inertial cavitation is produced by high acoustic intensities, thus these bubbles enhance thermal effect of HIFU and damage tissue mechanically with resultant shock waves and shear forces [56].

Ultrasound cavitation is pioneering method of cavitation in clinical application; yet there are some limitations and challenges [57]. Although some improvements have been promoted such as phased arrays probes, it is still troublesome to expose ultrasound precisely to the desired location due to phased aberrations and absorption induced by bones such as skulls and ribs. In addition, it is critical to apply ultrasound cavitation on delicate organs and parts of the body such as lungs, intestine, eyes and skin wounds not to change the physiology of the organs and cause burns and damages on the surrounding tissues because of lack of absorption of shock waves in the applies areas. The most important side effect of ultrasound cavitation treatments is hyperthermia. The cavitation applied tissue can be heated up to 80-100°C, consequently, coagulating necrosis occurs immediately at the spotted and the surrounding area as well [58], leading to various degrees of nerve and tissue damage.

Benign prostatic hyperplasia (BPH) is a frequently encountered disease in elderly male patients, caused by prostate tissue growth. Another disease, prostate cancer, is the cause of high morbidity and mortality in men. Besides conventional methods (i.e. surgery or androgen-ablative therapies), ultrasound cavitation becomes to be a wide-spread method against both benign and malignant cancers. However, it has still some side effects including rectal anal fistulas, urinary retention, incontinence, impotence, chronic pain and incomplete treatment of disease [59]. Owing to these drawbacks of ultrasound cavitation, hydrodynamic cavitation is a potential candidate to be an alternative therapeutic approach for abnormal tissue ablation. Since hydrodynamic cavitation is a cost effective, energy-efficient method which can be targeted the desired area easily. Hydrodynamic cavitation can destroy the desired area efficiently and precisely without any hyperthermia in the tissue; hence the side effects of heating are prevented in both the focused spot and the surrounding cells. Regarding to the advantages of hydrodynamic cavitation, we previously showed the destructive effect of hydrodynamic cavitation on leukemia cells [27]. In this study, we aimed to interrogate the feasibility and efficiency of hydrodynamic cavitation for biomedical applications

with further investigations. Therefore, we elucidated the demolishing effect of hydrodynamic cavitation on prostate cancer cells and BPH tissue. Its robust impact on cell death and tissue ablation points to promotion of a novel therapeutic method against cancer and tumor growth.

2 EXPERIMENTAL

2.1 Experimental Setup and Procedure for Hydrodynamic Cavitation

2.1.1 Materials and Methods

Hydrodynamic cavitation is the phenomenon, where inception, growth, and implosion of cavities are successively triggered in the body of a flowing liquid due to sudden changes in the fluid pressure. If a liquid flowing in a channel with a specific flow rate is forced through an orifice throat (Figure 4), the fluid velocity increases due to mass conservation.

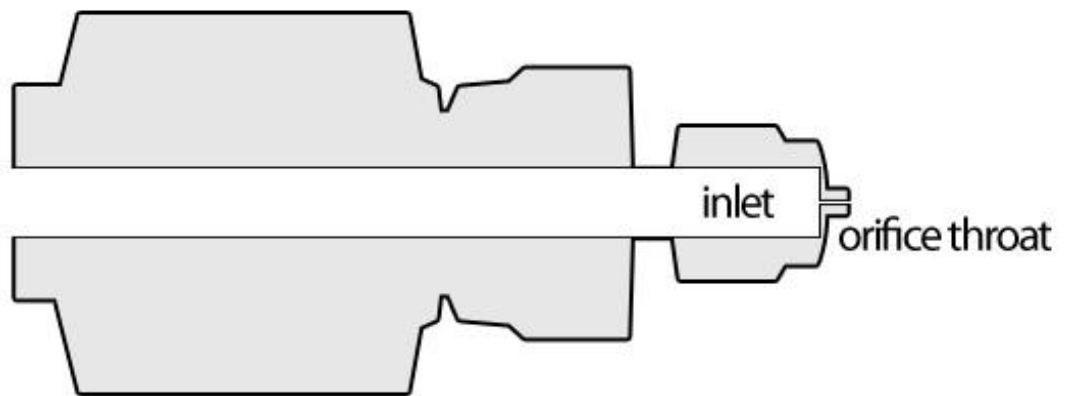


Figure 4 Microchannel configuration with the orifice throat and exit area

As the fluid velocity increases in a short micro channel (micro orifice), the pressure of the fluid decreases dramatically following the Bernoulli Equation. This decrease leads to sudden vaporization and formation of gas bubbles in the liquid at room temperature. The exit of the orifice could be subjected to ambient pressure, and emerging bubbly cavitating flow could be targeted onto the specimen. At that stage, the cavitation bubbles self-destruct and collapse inward. During the final stages of bubble implosion, the bubble wall velocity can reach or exceed the liquid sound of speed of sound, and shock waves are produced in the liquid [1] [14] [11]. These destructive effects can be exploited when applied on solid surfaces and lead to erosion on them.

The schematic of the experimental setup for generating bubbly cavitating flows is shown in Figure 5.

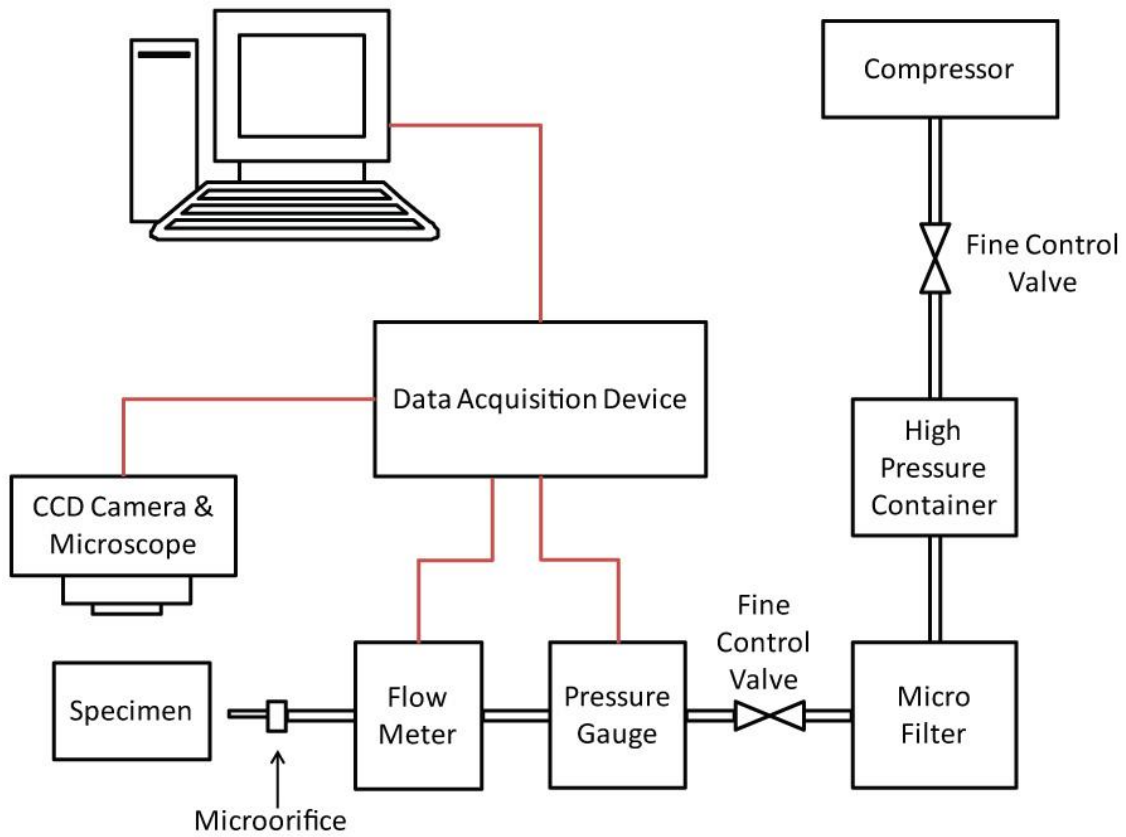


Figure 5 Experimental setup

A pressure driven flow follows the path in the schematic. When the fluid passes through a short micro probe, low pressures inside the microprobe are reached leading to formation of micro bubbles. [14] The micro bubbles emerging from the exit of the micro probe are targeted on various kidney stone samples. Hydrodynamic cavitation and emerging bubble motions are captured by Phantom v320 high speed camera.

This experimental setup is composed of a compressed air tank with controlled valve, pressure gauge with 6.8 kPa sensitivity, tubing, a high pressure Omega turbine flow meter with 0.011 ml/s sensitivity, and a fine control valve. Bubbly cavitating flows are generated using micro orifice geometry with a 0.75 cm long micro probe of 147 μm inner diameter. Orifice geometry was fabricated by laser drilling Polyether ether ketone (PEEK) tubes to obtain the desired inner diameters for the biomedical applications. PEEK material is a semi crystalline thermoplastic with good mechanical and chemical

resistance properties up to high temperatures. The material has great corrosion resistance and suitable for medical applications, which require sterile environment. [60]

2.1.2 Calcium Oxalate Real Kidney Stone Samples as a Model

Before the experiments, kidney stone samples were surgically removed in Demetevler Oncology Hospital, Ankara, and kept in saline solution at room temperature until experimentation. Surgically acquired kidney stones, which were taken from the same kidney, were classified according to their sizes. Similar stones have been selected to be analyzed by XRD (X-Ray Diffraction). Accordingly, XRD analyses of the 18 kidney stone specimens have shown that all the stones are composed of 90% calcium oxalate and 10% phosphate, whose material properties are included in Table 1.

Table 1 Material properties of calcium oxalate kidney stones. [61]	
Properties	Kidney Stone
Chemical Composition	Calcium oxalate monohydrate
Density (g/cm ³)	2.038
Young's Modulus (GPa)	24.51
Shear Modulus (GPa)	9.2
Poisson's Ratio	0.33

The experimental parameters have been adjusted in a controllable way to maintain effective hydrodynamic cavitation intensity (cavitation number $\sigma \sim 0.017$). Kidney stone sample to be tested was stabilized to a holder, and soft tape is placed between the kidney stone and the holder in order to avoid any disturbance on the specimen. Inlet pressures were adjusted to make sure to generate bubbly cavitating flow patterns at the desired intensity for destructive effects, while outlet pressure remained constant at atmospheric pressure (Figure 6).

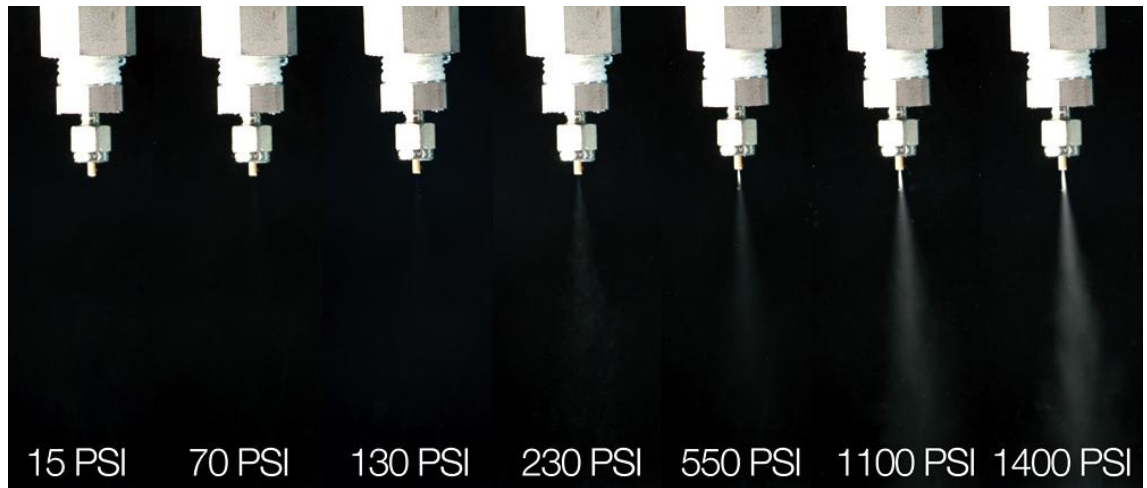


Figure 6 Visible cavitation cloud for the specified experimental setup inlets at inlet pressures between 50-70psi

Effective penetration depth caused by cavitating flows and the resulting destructive effect were highly dependent on the distance between the micro probe and the specimen (Figure 7).

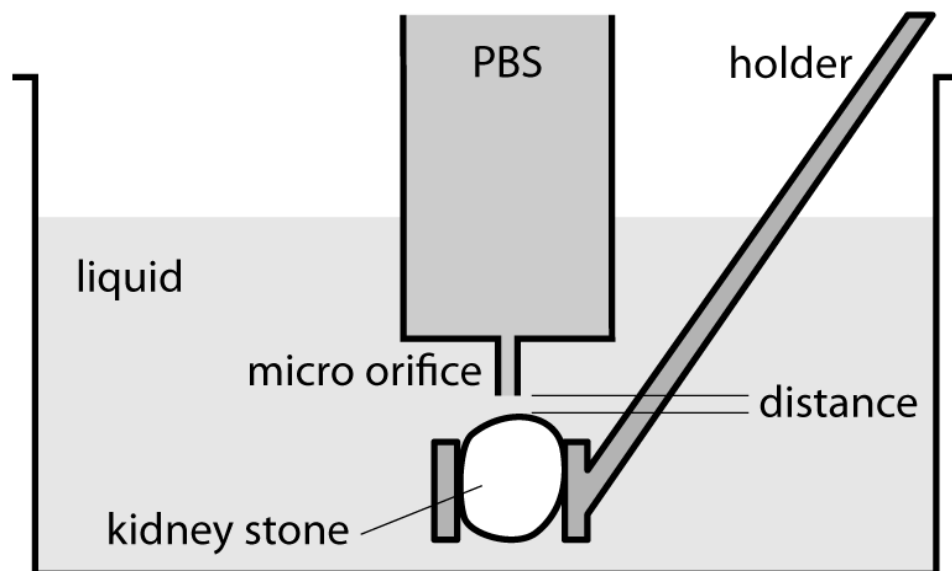


Figure 7 Experimental placement of the kidney stone.

1mm probe gap was selected as an optimal distance in the tests on kidney stone in parallel lines to our previous study. [27] Cavitation intensity is highly dependent on the

probe inner diameter, pressure and probe gap. We intended to use 147 μm inner diameter probe, which is suitable for both cavitation inception at moderate inlet pressures and visualization with the existing equipment. Small size of the probe provides more localized treatment. The diameter of the probe is selected to obtain the desired bubble size while the spacing between the probe and the specimen is determined in order to enhance bubble - specimen interaction and by taking the micro manipulator specifications into account.

The sterile conditions were sustained by autoclaving all the probes, orifice throat, containers, and valves before each test. Chemically and physically similar kidney stones were utilized for the cavitation experiments. The weight of each kidney stone specimen (listed in Table 2 with exposure durations) was measured before and after the experiments with 0.1 mg sensitivity.

Table 2 Kidney stone experiment sets. Fractured stones are marked with (*)				
	Mass at 0	Mass at 5 min	Erosion(g)	% Erosion at 5
Stone 1	0.0518 g	0.05 g	0.0018 g	3.47
Stone 2	0.0685 g	0.0669 g	0.0016 g	2.34
Stone 3	0.0526 g	0.0516 g	0.001 g	1.90
	Mass at 0	Mass at 10 min	Erosion (g)	% Erosion at 10
Stone 4	0.0751 g	0.0714 g	0.0037 g	4.93
Stone 5	0.0521 g	0.0509 g	0.0012 g	2.30
Stone 6	0.0918 g	0.0892 g	0.0026 g	2.83
	Mass at 0	Mass at 15 min	Erosion (g)	% Erosion at 15
Stone 7	0.0501 g	0.0479 g	0.0022 g	4.39
Stone 8	0.0548 g	0.0509 g	0.0039 g	7.12
Stone 9	0.0669 g	0.0642 g	0.0027 g	4.04
	Mass at 0	Mass at 20 min	Erosion (g)	% Erosion at 20
*Stone 10	0.0606 g	0.0562 g	0.0044 g	7.26
*Stone 11	0.0892 g	0.0848 g	0.0044 g	4.93
Stone 12	0.0714 g	0.0677 g	0.0037 g	5.18
	Mass at 0	Mass at 25 min	Erosion (g)	% Erosion at 25
Stone 13	0.0591 g	0.0548 g	0.0043 g	7.28
Stone 14	0.1104 g	0.101 g	0.0094 g	8.51
*Stone 15	0.101 g	0.0749 g	0.0261 g	25.84
	Mass at 0	Mass at 30 min	Erosion (g)	% Erosion at 30
Stone 16	0.0507 g	0.0455 g	0.0052 g	10.26
*Stone 17	0.1301 g	0.1182 g	0.0119 g	9.15
Stone 18	0.1182 g	0.1094 g	0.0088 g	7.44

After each test, eroded kidney stones were placed to a sterile container kept at room temperature and were left for drying for a day. Thereafter, the weights of the specimens were measured again so that erosion amounts could be assessed.

For assessing the erosional effects caused by hydrodynamic cavitation on kidney stones control experiments were performed. These experiments were considered to use the same outlet velocity for both cavitating and non cavitating conditions. For a small amount of time (around 2 minutes), no significant erosional change was observed in control experiments with the same outlet velocity. It was observed that the erosion on the tested stones resulted because of the bubbles rather than high speed shear flows. Moreover, the flow rate value was also fixed to maintain comparable results for the real and control experiments. The experiments were conducted with a probe having a larger inner diameter (2.8 mm). The flow rate was kept as the same (1.9 ml/s) as under cavitating flow conditions and the experiments were conducted for each time value. The obtained results were recorded and compared to the cavitating conditions. It was observed that no significant erosion on kidney stone samples was present after the control experiments, which were conducted under non-cavitating conditions. A similar experimental setup placing a kidney stone in a finger tip size container with 5cc volume was prepared to compare freely rotating kidney stones with stationary stones during the application of bubbly cavitation. Freely moving stones were exposed to bubbly cavitation with the same intensity. Under these conditions, the initial and final weights of the samples were measured. The erosion on the rotating stones had the same linear trend as the stationary stones. Therefore, the change of the exposed area on the stone did not affect the total erosion amount on the exposed sample.

2.2 Experimental Procedure for Prostate cells and Tissue

2.2.1 Cell line, cell culture and treatments

PC-3 human prostate adenocarcinoma cells and DU-145 human prostate carcinoma cells were cultured in Dulbecco's modified Eagle's medium (DMEM; Biological Industries) supplemented with 10% (v/v) fetal bovine serum (FBS; **PAN, P30-3302**), 2 mM L-glutamine and antibiotics (100ug penisilin/100U streptomycin; Biological Industries, 03-031-1B) in a 5% CO₂-humidified incubator at 37°C.

PC-3 and DU-145 cells were treated with 8 μM Staurosporine (Sigma, #S5921), 10 μM Cisplatin (Sigma, #P4394) and 50 μM Etoposide (Sigma, # E1383) as positive controls for apoptosis activation and cell cycle arrest tests, respectively.

2.2.2 Experimental set-up and procedure

All experiments were done with the experimental set-up as previously described in kidney stone experiments. A schematic of experimental apparatus is shown in Figure 5.

The liquid (1X PBS) flows through the tube by pressure pump. Cavitating bubbles are formed in the chamber due to local pressure drop. Emerging bubbles expand at the end of the microprobe and targeted to the desired spot. All equipments and solutions were sterilized with 70% ethanol and autoclave. Microorifice was cleaned by sonication and sterilized with 70% ethanol. A physiological solution (PBS) was used as a liquid environment to produce cavitation.

A pressure driven flow occurs through a 10 mm long PEEK (polyether ether keton) probe with an inner diameter of 147 μm , which generates a flow restrictive orifice leading to low local pressures. PEEK material provides good mechanical and chemical resistance even at high temperatures and has great corrosion resistance and compatibility to medical applications. The experimental pressure values for inlet of the orifice were between 50 PSI and 150 PSI. The exit pressure of the orifice was set to atmospheric pressure, which provides a similar ambient pressure for in vivo applications. In the experiments, the inlet pressure was increased until cavitating flow conditions were observed. Thereafter, the inlet pressure was set to the desired value while ensuring to maintain cavitating flow conditions. Bubble cloud and bubble emergence at the exit of the orifice was captured by a double frame Phantom V320 high speed camera along with a light microscope unit and a image processing software.

2.2.3 Cavitation Pressure Kinetics and Exposure Time Kinetics Experiments

Prostate cells; PC-3 and DU-145; were trypsinized and splitted into 75 cm^2 flasks at a cell concentration of 1×10^6 cells/ml. Hydrodynamic cavitation was applied onto cells for different exposure times; 1 minute, 2, 3 and 5 minutes and under different

inlet pressures; 50, 100 and 150 PSI for pressure kinetics experiments while the outlet pressure (pressure in the solution) was kept as atmospheric pressure. After cavitation exposure, cells were collected into falcons and centrifuged at 300 g for 5 min and cultured for 24 hours.

2.2.4 Cell counting and Cell Death Analysis of Cavitated Samples

After the cavitation experiment, the cells were centrifuged at 300 g for 5 minutes, carefully washed and resuspended with a fresh medium. Cell viability was determined by trypan blue (Sigma, #T8154) exclusion assay and cell numbers were counted in a hemocytometer under light microscope after 0 (just after cavitation) and 24 hours of culture following exposure to cavitation.

2.2.5 Cell Cycle Analysis

PC-3 cells were cultured for 0, 6, 12 and 24 hours after cavitation (150 PSI, 5 min). At indicated time points, cells were trypsinized and centrifuged at 1200 g for 5 min at room temperature. Following to washing cells with PBS, cells were fixed with ice cold 70% ethanol at -20 °C till the end of time points. Ethanol was discarded after centrifugation and cells were resuspended with PBS. Cells were treated with 100 µg/ml RNase A (Sigma, # R6513) for 30 min at 37 °C. Propidium iodide (PI) (Invitrogen, # P3566) was added to the cell suspension at a final concentration 40 µg/ml and incubated for 30 min. The cells were then analyzed by flow cytometry using FACScan (Becton Dickinson). The results were quantified by using the software Cell Quest (Becton Dickinson).

2.2.6 DNA Fragmentation Assay

Genomic DNA isolation from cavitation exposed and non-exposed PC-3 cancer cells are isolated as described previously (*Hermann M. et al, 1994*). After cavitation, suspended cells were harvested by centrifugation at 1500 g for 5 min at 4°C. Cells were lysed in lysis buffer (1% NP-40, 20mM EDTA and 50mM Tris-CL, pH: 7.5) for 10 seconds. After centrifugation (1600 g for 5 min at 4°C), supernatants were transferred into new eppendorf and incubated at 56°C for 2 hours after addition of 1% SDS and 0.5 µg/µl RNase A. Afterwards, Proteinase K (Promega, # V3021) treatment (with final concentration 5 µg/µl) was performed at 37°C for at

least 2 hours. Following to precipitation of DNA with $\frac{1}{2}$ V 10M ammonium acetate and 2.5 volume % 100 ethanol, DNA samples were washed with 70% ethanol. DNA samples were run in 2% agarose gel to separate the DNA fragments.

2.2.7 Cavitation Experiments on Human Benign Prostatic Hyperplasia (BPH) Tissue

Human Benign Prostate tissues are obtained from Maltepe University Hospital in a sterile container. PBS was used as a liquid environment for generating cavitating bubbles. Bubbly cavitation under 100 bar pressure (1450 PSI) was exposed onto the BPH tissue for 15 and 20 min, while the outlet pressure (pressure in the solution) was kept as atmospheric pressure. To demonstrate the effect of cavitation more than shear effect, cavitation control was applied to the tissue. This control test was accomplished via exposing liquid with same flow rate as cavitation without generating cavitation bubbles. After cavitation, the cavitation exposed area was labelled with green tissue dye and the tissues were fixed in %10 formaldehyde solution for 24 hours. The tissues were cut longitudinally along the cavitation line in order to get more information about cavitation depth.

2.2.8 Hematoxylin and Eosin Staining

After routine tissue processing (Shandon Excelsior) the prostate tissues were embedded in paraffin. 4 μ m thick tissue sections were obtained from the paraffin blocks, deparaffinized in xylene and rehydrated through a graded ethanol series (3x5 min). Afterwards, tissue sections were stained with hematoxylin and eosin (H&E) dye. The BPH tissue samples were examined and evaluated by a pathologist under blindfold conditions with standard light microscopy (Olympus BX51).

2.2.9 Statistical Analysis

The student's test was used to analyze the statistical difference between control, cavitation non-exposed, group of each time points and cavitation exposed samples. Values of $p < 0.05$ were considered significant.

3 RESULTS AND DISCUSSION

3.1 Results and Discussion of Hydrodynamic Cavitation Study

3.1.1 Results and Discussion of Kidney Stone Experiments

Figure 8 displays flow rates as a function of inlet pressures. The flow rate has an increasing trend with inlet pressure as can be seen from this figure. At higher inlet pressures, the slope of the trend decreases indicating the arrival of choked flow conditions, which were also reported in the literature about hydrodynamic cavitation in micro scale. [62]

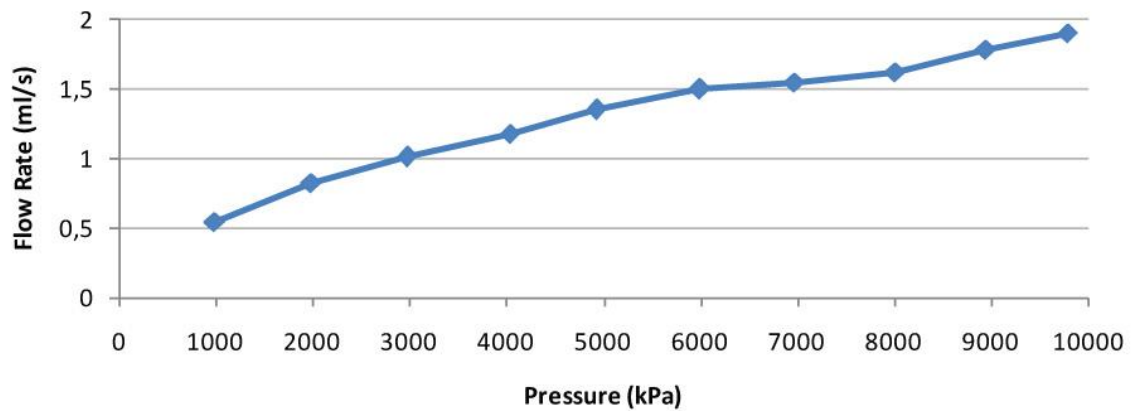


Figure 8 Volumetric flow rates as a function of inlet pressure. (Cavitation is observed over the entire range of pressure)

During the experiments, it was observed that cavitation incepted at a pressure of ~992 kPa. By increasing the pressure beyond this point more distinct bubble clouds were observed (Figure 9). The emerging micro bubbles from the exit of the micro probe were recorded by the high speed camera, and the bubble sizes were measured using captured images. The size of the micro bubbles targeted to the samples varied from 60 μm to 300 μm .

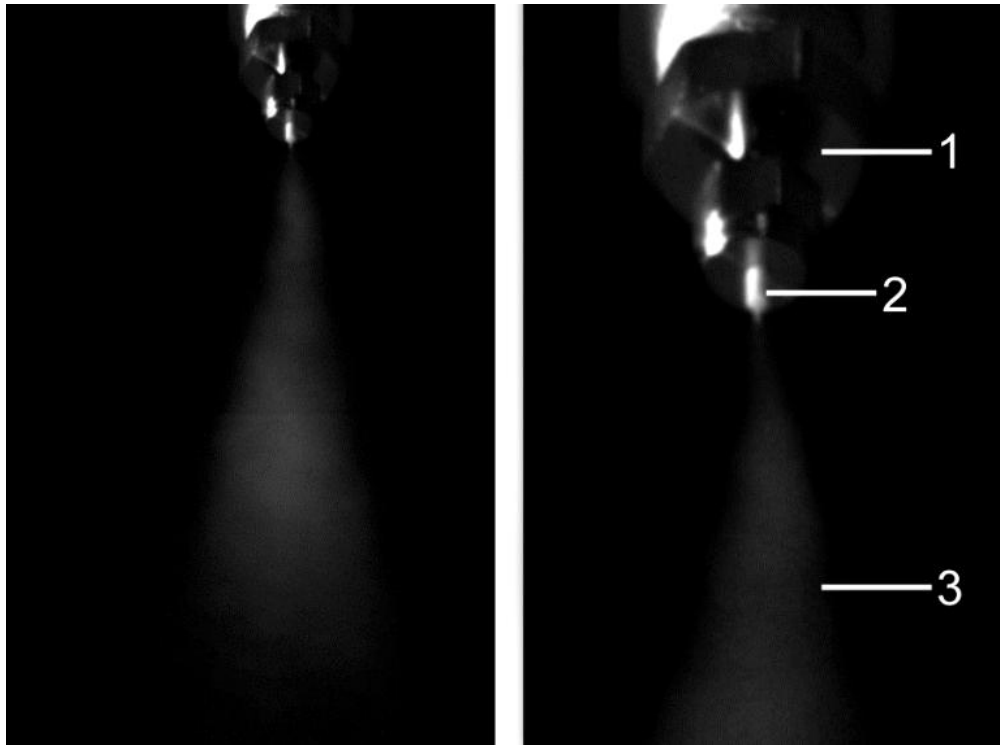


Figure 9 Cavitation bubble cloud images captured by the high speed camera. (1) Inlet. (2) Micro probe (Orifice throat) (3) Bubble Cloud.

The maximum pressure value was imposed by the maximum available pressure for the present experimental setup measured as 9790 kPa. Under the conditions of the maximum applied pressure, the flow rate was measured as 1.9 ml/s, while the corresponding cavitation number was deduced as $\sigma \sim 0.017$. This value lies within the range of the existing micro scale cavitation studies. [63]

The erosional effects of hydrodynamic cavitation have been assessed by comparing the initial weights of kidney stones to their final weights. Furthermore, the resulting kidney stone damage was also visually monitored. After the experiments, eroded kidney stones showed a more porous structure, and their volumes were visibly reduced. Their shape also became more spherical as shown in Figure 10 Bubble-kidney stone interactions lead to a more regular and porous shape.

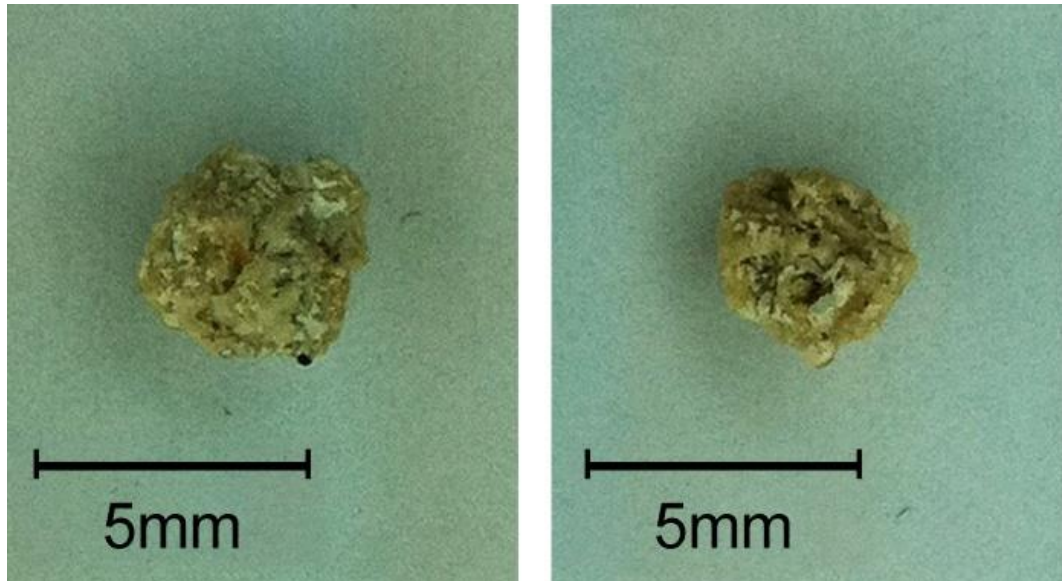


Figure 10 Kidney stone before exposure to bubbly cavitation. (b) Erosion on kidney stone after exposure to bubbly cavitation.

As can be seen from **Figure 11**, a linear relation between erosion amount and time can be observed. If however the stone sample is broken during the experiment, the profile diverges from this linear trend (Stones 10, 11, 15, 17) as indicated with black circles.

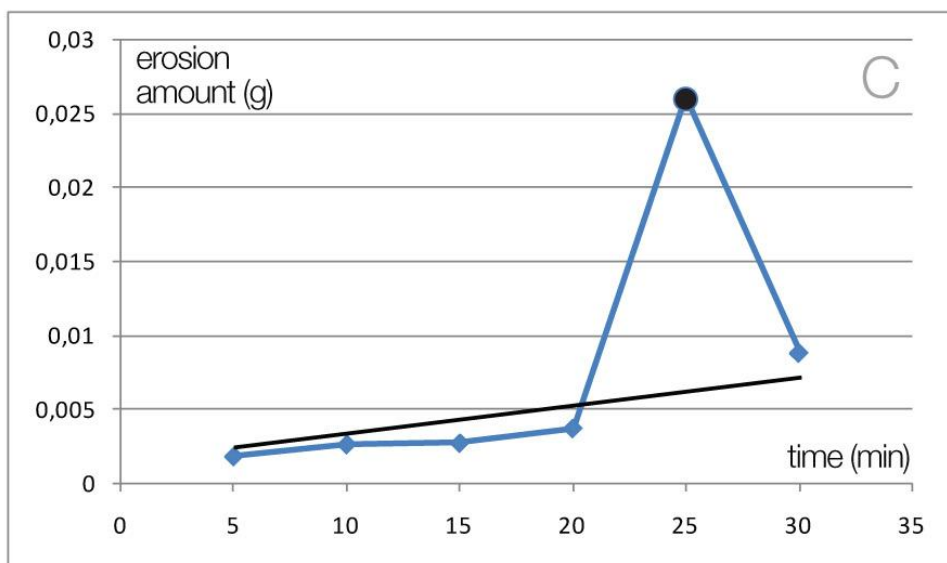
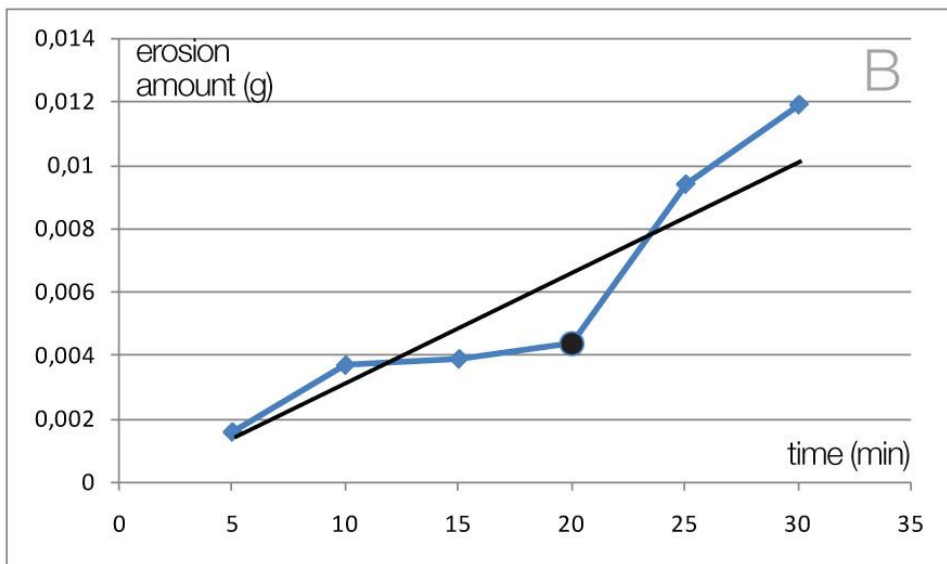
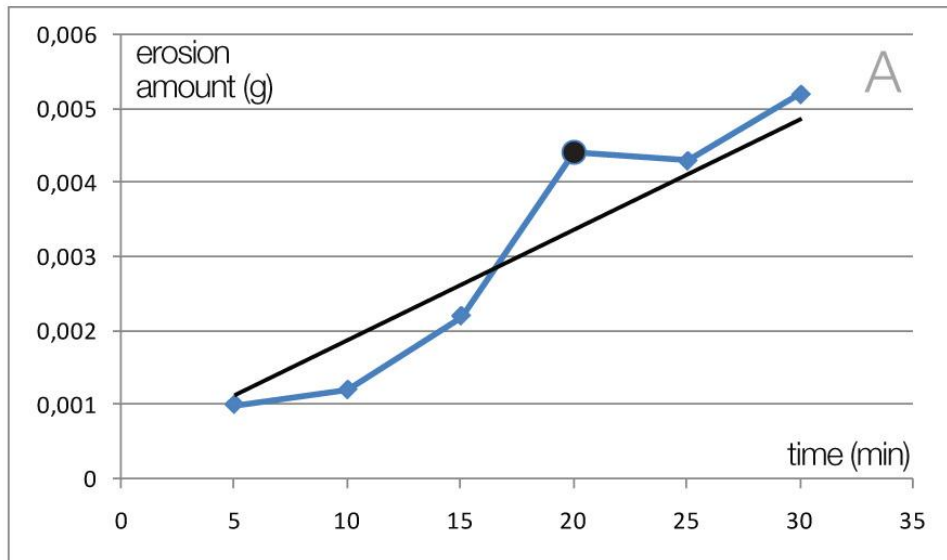


Figure 11 (a), (b) and (c). Experimental results of kidney stone as a function of time (min). Broken stones are marked with black circle.

When the kidney stone sample breaks, almost two equivalent halves are formed along with many small particles (debris, Figure 12), which can easily go through the urinary tract and were therefore not considered when measuring the final weight of the treated kidney stone sample. The total mass of the small particles and debris accounts for a significant portion of the final weight. Because this portion is not taken into account, a jump in the erosion amount and diversion from the linear trend occur upon the fracture of kidney stone samples.

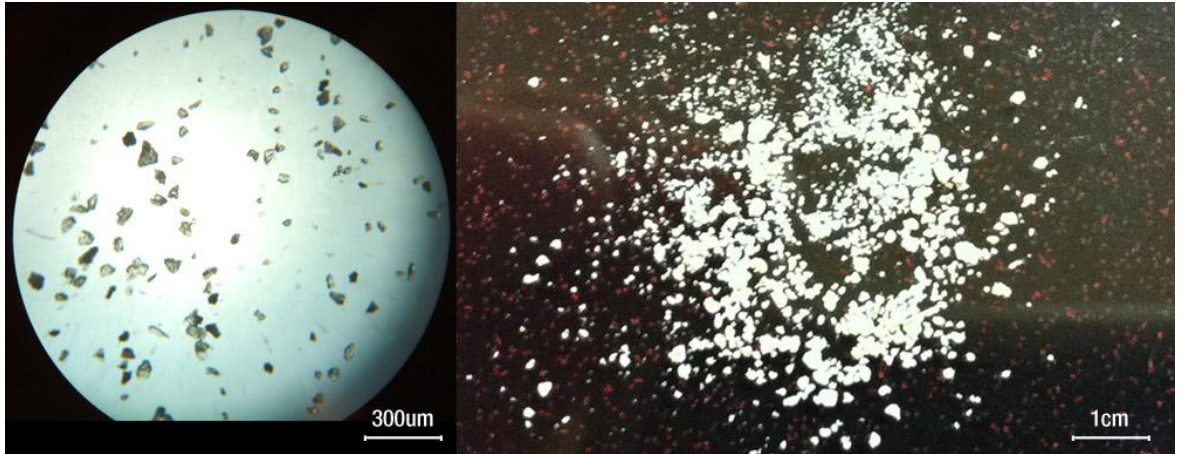


Figure 12 Stone debris

In an attempt to develop a general prediction tool for the average erosion rate on calcium oxalate based kidney stones caused by hydrodynamic cavitation, Sheldon and Finnie's 90° brittle erosion model [64] recommended for brittle surface materials is utilized as the reference. In this model, erosion is considered as removal of surface material by the cumulative actions of individual particles. Calcium oxalate based kidney stones are brittle and thus cannot deform elastically. Instead, they crack and fracture when subjected to tensile stress. The angle of maximum erosion for brittle materials is close to 90°. [1] Accordingly, erosion rate is expressed in this model for spherical particles, which are considered as micro bubbles in this study, as:

$$W = C_e R_p^\xi V^\eta \quad (1)$$

$$\xi = 3f/(f - 2) \quad (2)$$

$$\eta = 2.4f/(f - 2) \quad (3)$$

$$C_e = E_t^{0.8} \sigma_b^2 \quad (4)$$

where R_p is the particle radius (average bubble radius, 180 μm in this study), σ_b is the flexural strength, V is the particle velocity, and E_t is the Young's modulus of elasticity. Using the average erosion rate of 0.31 mg/min found in the results on erosion rates in this study and assuming that micro bubbles emerging from the microprobe have the same velocity as the flow velocity inside the microprobe, this model supplies a friction coefficient (f) value of 2.65. This value could be utilized as the input for Eq. (1) so that Eq. (1) could be employed to estimate the average erosion rate on calcium oxalate based kidney stones exposed to hydrodynamic cavitation leading to micro bubbles of size R_p and flow velocities V at the microprobe cross section.

Despite the fractures in some kidney stone samples, the average erosion amount demonstrates a linear trend with time (Figure 13). Accordingly, an average material removal rate of 0.31 mg/min is obtained from the experiments (Figure 13a). It can also be seen that no significant change in the mass of kidney stone samples is apparent after the control experiments suggesting that major erosion was caused by bubbly cavitating flows rather than shear forces caused by pure fluid jet flows. The corresponding average changes in mass percentages for kidney stone samples are included in Figure 13b. Erosion percentages up to 10% could be attained within half an hour with the proposed method. Moreover, 4 out of 18 kidney stones were broken within short time proving the effectiveness of the proposed method.

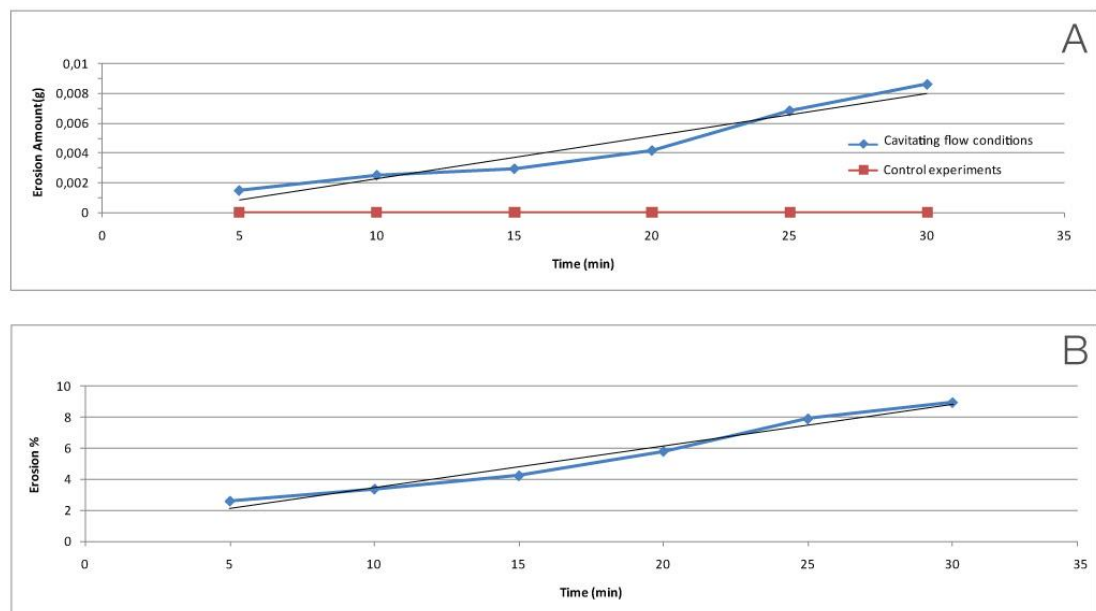


Figure 13 (a) Average erosion amount (g) vs. time (min) graph at 9790 kPa pressure, 1mm probe gap. Bubbly cavitation sets are at the top. Control experiments are

at the bottom. (b) Average erosion amount (in %) vs. time graph at 9790 kPa pressure, 1mm probe gap.

A similar experimental setup placing a kidney stone in a finger tip size container with 5cc volume was prepared to address that change. Freely moving sample was exposed to bubbly hydrodynamic cavitation of the same intensity. The stone was confined but free to rotate. (Figure 14, Figure 15) Under these conditions, the initial and final weights of the samples were measured. (Figure 16) The erosion on the stones had a linear trend. Therefore, the change of the exposed area on the stone did not affect the total erosion amount on the exposed sample.

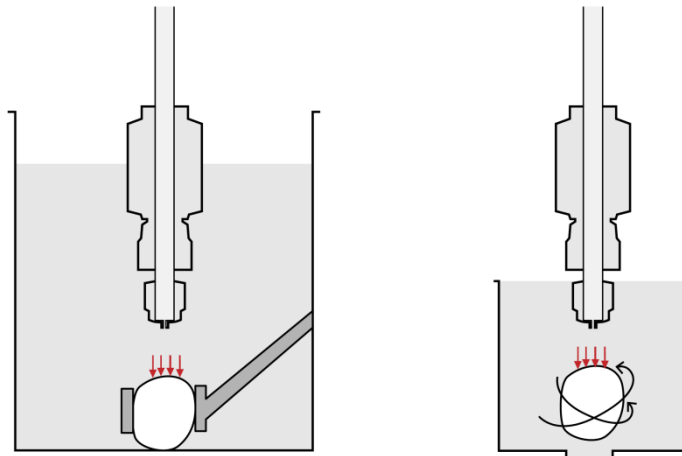


Figure 14 (a) Stabilized sample (b) Free rotating sample in 5cc container



Figure 15 (a) Erosion in bubble path direction for stationary sample (b) Erosion in every direction for rotating sample

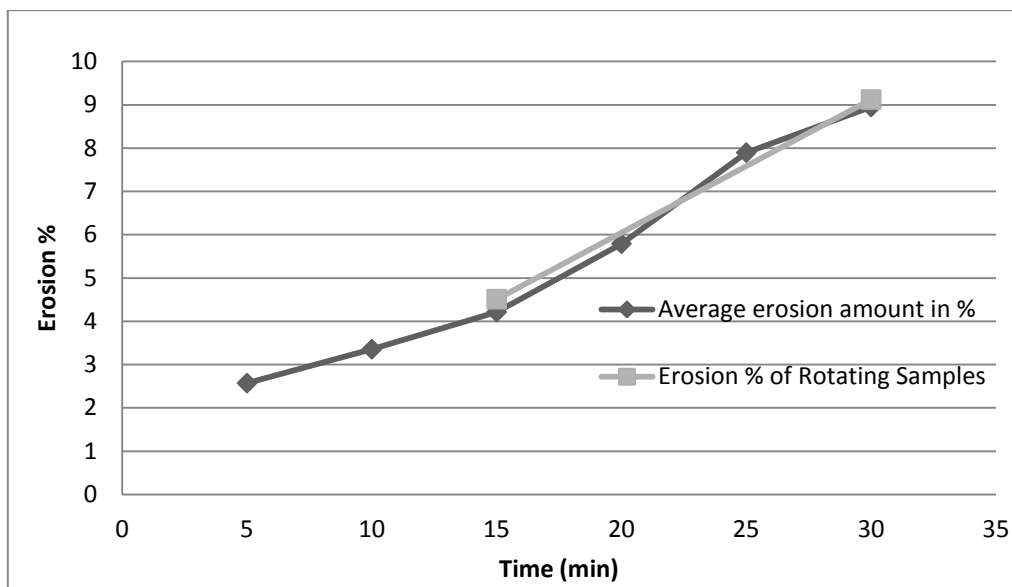


Figure 16 Average erosion amount for stationary samples (in %) and erosion amount for stationary samples (in %) vs. time graph at 9790 kPa pressure

3.1.2 Results and Discussion of Prostate Cells and Tissue Experiments

To identify the effect of hydrodynamic cavitation on human cell lines, bubbly cavitation was exposed to PC-3 (human prostate adenocarcinoma cell line) and DU-145 (human prostate carcinoma cell line) cells *in vitro*.

Hydrodynamic cavitation was applied on PC-3 and DU-145 cells with a spectrum of different pressures; 50, 100 and 150 PSI. To check the reaction of cells against cavitation, they were harvested for 0 and 24 hours following to cavitation. Cell numbers and cell death ratios were determined before, immediately after cavitation exposure (0 h) and at the end of incubation time (24 h). In these experiments, cell death observed after cavitation (0 h) did not exceed 10 % of total cell number in both cell lines (Figure 2 a, b). Also, cell death ratios did not increase 24 h after cavitation. Late effects of cavitation were not detected, even after 24 hours. As a result, all cells encountering bubbles exploded leaving behind only undamaged cells with intact membranes, hence trypan blue negative. Nevertheless, under microscope, the number of cells after cavitation exposure was dramatically decreased. It demonstrated that cavitation killed a significant proportion of cells in both two different cell lines. Therefore, cell numbers were counted following application of different exposure pressures.

The cell number counts demonstrated that amount of intact cells significantly decreased after cavitation exposure in both PC-3 and DU-145, and this reduction in cell numbers was positively correlated with the applied pressure. Just after cavitation, bubbly cavitation with 150 PSI pressure decreased the number of intact cells among PC-3 and DU-145 cells to 50% and 30 % of the initial cell numbers, respectively (Figure 2 c,d). In addition, although there was no increase in cell death after 24 h, cavitation exposed cells, especially 150 PSI, and exposed samples did not grow as fast as control (cavitation non-exposed) cells. All these results showed that under optimized pressure condition hydrodynamic cavitation caused a robust cell death effect independently from cell type, leading to the destruction of all damaged cells.

To better characterize cavitation effects and to establish a exposure time correlation, cavitation was applied with different exposure times; 1, 2, 3 and 5 minutes. The pressure was set to 150 PSI which represented the effectiveness of cavitation vigorously. Cell numbers and cell death ratios were determined immediately after cavitation exposure (0 h) and at the end of incubation time (24 h). Like pressure kinetics experiment, cell death ratios observed after cavitation (0 h) were not higher than 12 % of total cell number in both PC-3 and DU-145 cell lines (Figure 17 a, b). Also this percentage did not increase over time, after 24 hours. On the other hand, cell numbers after cavitation exposure was reduced significantly (Figure 17 c, d).

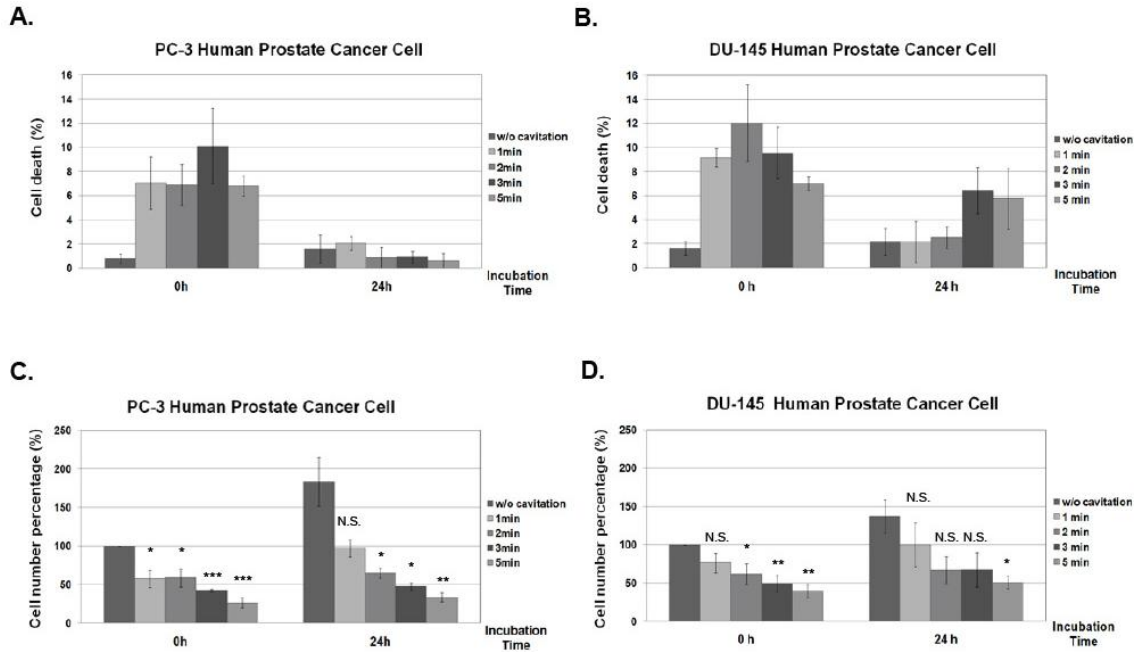


Figure 17 Hydrodynamic cavitation caused a dramatic decrease in cell number in an exposure time dependent manner. Hydrodynamic cavitation exposed on prostate cancer cells; PC-3 and DU-145 under an inlet pressure of 150 PSI for 1, 2, 3 and 5 minutes. Control samples were unexposed to cavitation. Cell death ratio of A) PC-3 and B) DU-145 and cell numbers of C) PC-3 and D) DU-145 were determined after cavitation (0 h) and 24 hours later. Cell death was analyzed via trypan blue exclusion assay and cell numbers of each sample were normalized to values of control sample at 0 h. Data are shown as mean \pm S.D (n=3, Student t-test * $p < 0.05$, ** $p < 0.01$, *** $p < 0.001$).

The cell number percentages declined in an exposure time dependent manner and after 5 minutes cavitation application just 25-30 % of total cells were alive in both two cell lines. The growth rate of the cells after cavitation was not high. Thus the number of the cells did not increase after 24 h as much as cavitation non-exposed cells. The growth rate difference, between cavitation non-exposed and exposed cells was more obvious in PC-3 cells. While cavitation non-exposed cells doubled their numbers over 24 h (from 100% to 183%), the number of cavitation exposed cells was more or less same.

Previously, in vitro studies showed that ultrasound cavitation kills cells immediately or damages cell membrane and induce cell death mechanisms [32]. To determine the hydrodynamic cavitation induced death mechanisms, apoptosis activation

is investigated. Apoptosis is the main programmed cell death mechanism in multicellular organisms. While apoptosis is morphologically characterized by membrane blebbing, cellular shrinkage, chromatin condensation and formation of apoptotic bodies, biochemically its main features are caspase activation and DNA fragmentation. Therefore, we checked caspase activation and PARP cleavage. Caspases are proteases and activated by proteolytic cleavage by each other. Activated executor caspases are cleaves some cytoplasmic and nuclear proteins give rise to the apoptotic death morphology. PARP is one of the nuclear proteins. Therefore, its cleavage could indicate apoptotic activation.

The activation of initiator caspase, caspase-8 and executor caspase, caspase 3 and PARP cleavage were determined via western blot analysis. The activation of apoptosis in cavitation non-exposed and exposed cells was evaluated compared to apoptosis induced samples like staurosporine or cisplatin treated cells. According to western blots, in both PC-3 and DU-145 cell line, either pressure kinetics or exposure time kinetics samples did not activate apoptosis (Figure 18 a and b).

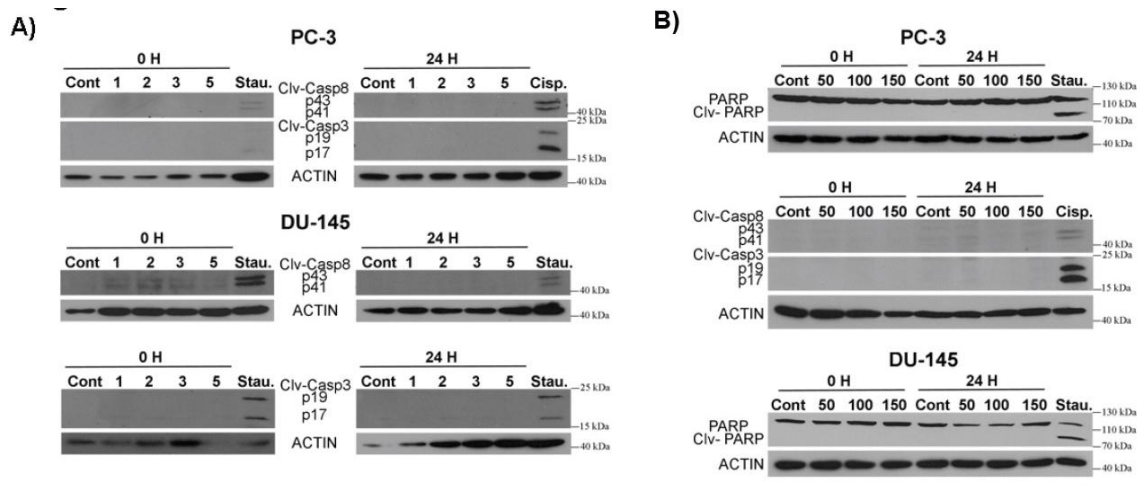


Figure 18 Apoptotic activity was not induced following to hydrodynamic cavitation exposure on prostate cells. No PARP cleavage and caspases activation was checked after cavitation. Hydrodynamic cavitation effect on prostate cancer cells; PC-3 and DU-145 A) with a pressure kinetics (50, 100 and 150 PSI) at a constant exposure time (5 min) was checked by means of apoptotic activity at 0 h (immediately after cavitation) and 24 hours after cavitation. Control samples were unexposed to cavitation. 8 μ M Staurosporine and 10 μ M Cisplatin treated samples are used as positive control for apoptosis activation.

There were no caspase 8 and 3 activation and their downstream effect, PARP cleavage, neither at 0 and nor at 24 hours. These results further supported that hydrodynamic cavitation killed majority of cells and the remaining ones tried to overcome this stress condition without any late effect including undergoing apoptotic cell death.

Autophagy (from the Greek, “auto” oneself, “phagy” to eat) is an evolutionarily conserved self-digestion mechanism which provides a critical adaptive response against stresses conditions. Autophagy acts as a survival mechanisms via retarding or preventing apoptosis [65]. On the other hand, under some conditions it may induce caspase-independent type II programmed cell death, namely autophagic cell death [66] [67] [68].

Autophagy activation was checked using p62 and LC-3 immunoblots. These two proteins are commonly used as autophagy markers. p62 takes role for the packing and delivery of polyubiquitinated, misfolded and aggregated proteins to the autophagic

pathways for their clearance. The amount of p62 decrease reflects the enhanced autophagic activity. LC3 protein is the most widely used autophagy marker since the conjugated form resides on the autophagic double membrane. LC3 is found in a free nonlipidated form in cytoplasm, called as LC3I. During autophagy, LC3I (18kDa) is conjugated to the lipid, phosphatidylethanolamine (PE), and forms the lipidated form known as LC3II (16kDa). The size differences of these two forms provide the detection of autophagy in protein level detections. The shift from LC3-I to II indicates autophagy induction.

Hydrodynamic cavitation did not induce autophagy immediately after cavitation as well as 24 hours later (Figure 5). There was neither p62 degradation nor LC3-II shifting detected. This results were obtained in both cell lines proving the cell independent effect of hydrodynamic cavitation.

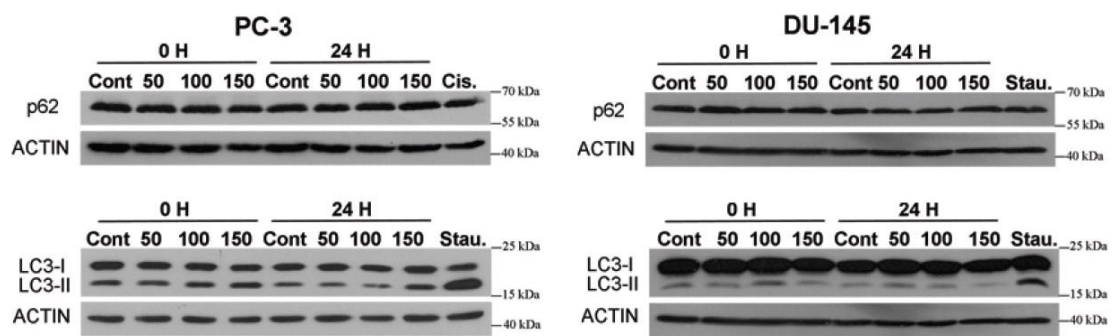


Figure 19 Hydrodynamic cavitation did not induce autophagy. Autophagic activity was checked with p62 degradation and LC3-I to II shifting. Hydrodynamic cavitation impact on prostate cancer cells; PC-3 and DU-145 with a pressure kinetics (50, 100 and 150 PSI) at a constant exposure time (5min) was controlled by means of autophagy at 0 h (immediately after cavitation) and 24 hours after cavitation. Control samples were unexposed to cavitation. 8 μ M Staurosporine and 10 μ M Cisplatin treated samples are used as positive controls.

Hydrodynamic cavitation exposure results in dramatic cell number decrease without any change in detectable cell death ratios. While any late effect is detected in 24 hours following to cavitation exposure, the cell number does not increase in cavitation exposed cells as much as control, cavitation non-exposed, cells. Also, the cell death ratios does not increase by time. Therefore, to understand whether there is arrest during the cell cycle as a result of hydrodynamic cavitation, cell cycle stages were checked

among the cells. Cell cycle arrest results demonstrated that hydrodynamic cavitation did not cause any reasonable change in the cycle of cell division, and no cycle arrest was identified (Figure 20 a).

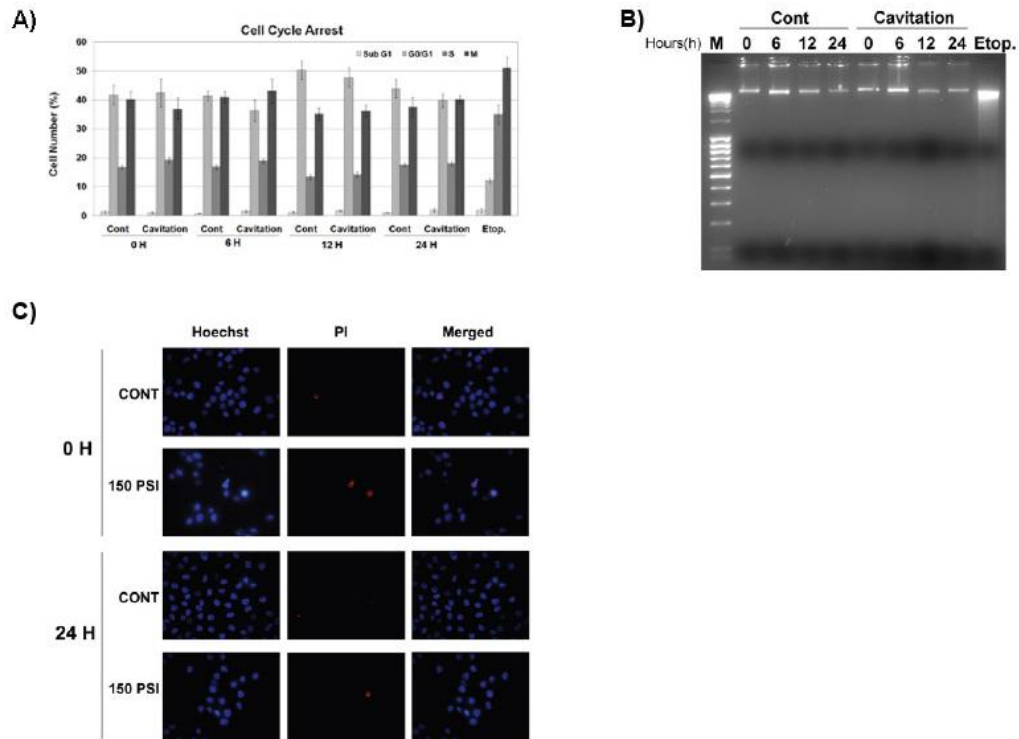


Figure 20 The reduction of cell growth following to hydrodynamic cavitation was not caused by neither cell cycle arrest nor DNA fragmentation. PC-3 cells were exposed to 150 PSI, 5 min cavitation and cultured for 0, 6, 12 and 24 hours. Control samples were unexposed to cavitation. A) There was no difference in cell cycle of cavitation exposed cells in comparison to cavitation unexposed cells. Cell cycle arrest analysis of PC-3 was performed by flow cytometry at 0, 6, 12 and 24 hours after cavitation. Etoposide, positive control, treatment caused cells arrest in M phase. Data are shown as mean \pm S.D (n=3). B) Hydrodynamic cavitation did not cause any DNA breaks leads to DNA fragmentation. Cavitation samples did not have any fragmented DNA as well as cavitation unexposed control samples. C) 50 μ M Etoposide treatment for 24 hour was done to assess the methods with positive control sample.

No difference was detected between control and cavitation exposed cells in terms of behaviours in cell cycle within 24 hours after cavitation. In fact, it was observed that cavitation exposed cell continued to divide slower than cavitation non-

exposed cells even 48 hour after exposure. Apart from the cell cycle arrest, DNA integrity was checked to enlighten the idea of deceleration of growth rate due to cavitation induced DNA damage. Hydrodynamic cavitation did not neither demolish DNA even just after exposure nor induce DNA fragmentation as a late effect (Figure 20 b, c). Chromatin integrity was intact and chromatin condensation, which is one of the features of apoptosis, was not examined as a consequence of cavitation. Like PARP cleavage and caspase activation tests, these results also indicate that hydrodynamic cavitation does not induce apoptosis. In addition, hydrodynamic cavitation did not induce any breaks in DNA which was checked by activation of H2Ax phosphorylation that is a guidance for activation of DNA repair mechanisms. The effect of hydrodynamic cavitation on cell growth is not caused by any defect in DNA and cell cycle as well.

Following to the human cell lines, the destructive effect of cavitation was tested on human tissues to have an idea about its feasibility in clinical application. To achieve this goal, cavitation with higher inlet pressure 1450 PSI (approximately 100 Barr) was immediately applied onto the BPH tissue for 15 and 30 minutes (around 1-1.5 hrs after the surgical operation). Hydrodynamic cavitation incorporates both the bubble implosion energy and the shear effect of the liquid flow. To assess the contribution of the shear forces to tissue ablation some control experiments were also performed. The liquid jet was directed to tissue with same flow rate, yet different pressure from cavitation. The effect of cavitation on tissue was determined by histopathological analysis following hematoxylin and eosin staining.

In comparison to the normal human prostate tissue, there was obvious tissue damage in the cavitation area (just around the targeted region) (Figure 21).

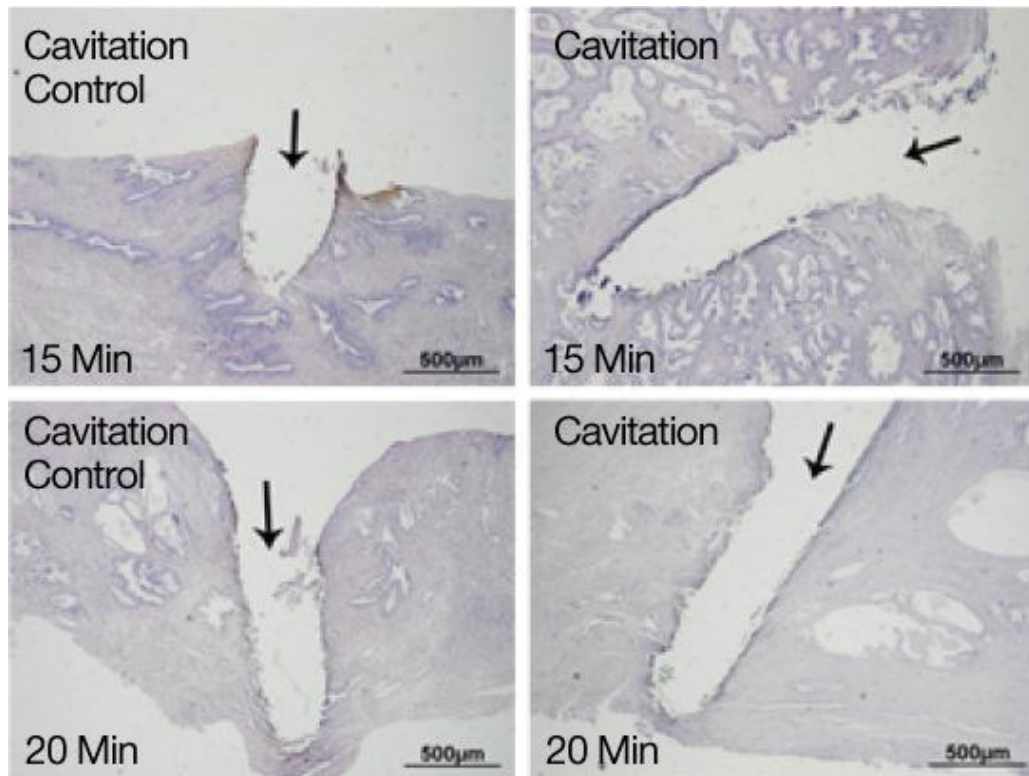


Figure 21 Hydrodynamic cavitation eroded the human BPH tissue effectively and precisely. A) Cavitation control (at same flow rate, yet different pressure with cavitation) and cavitation (1450 PSI) exposed BPH tissues for 15 and 30 minutes were observed under 40X. Histopathological analysis was done with H&E staining.

Although cavitation control resulted in a cavity in tissue due to shear force, the cavitation exposed tissue areas had a deeper cavity. This demonstrated that bubbly cavitation, rather than the shear effect of the liquid flow, is the actual cause of cell death or tissue ablation in cavitation experiments. Furthermore, like cell line experiments, the demolishing effect of hydrodynamic cavitation was exposure time dependent. All cells at the targeted region were killed, and as a result, a cone shaped cavity was formed at the cavitation exposed area (arrows). On the other hand, no clear cell death, necrosis or karyolysis at the surrounding area of cavitation spot was observed.

These results demonstrate how hydrodynamic cavitation could precisely be targeted to a desired area without giving any harm to the surrounding healthy cells or tissues, and how it could destroy targeted area. This clearly provides valuable proof for its potential as a treatment method for biomedical applications; especially against abnormal tissue growths.

4 CONCLUSION

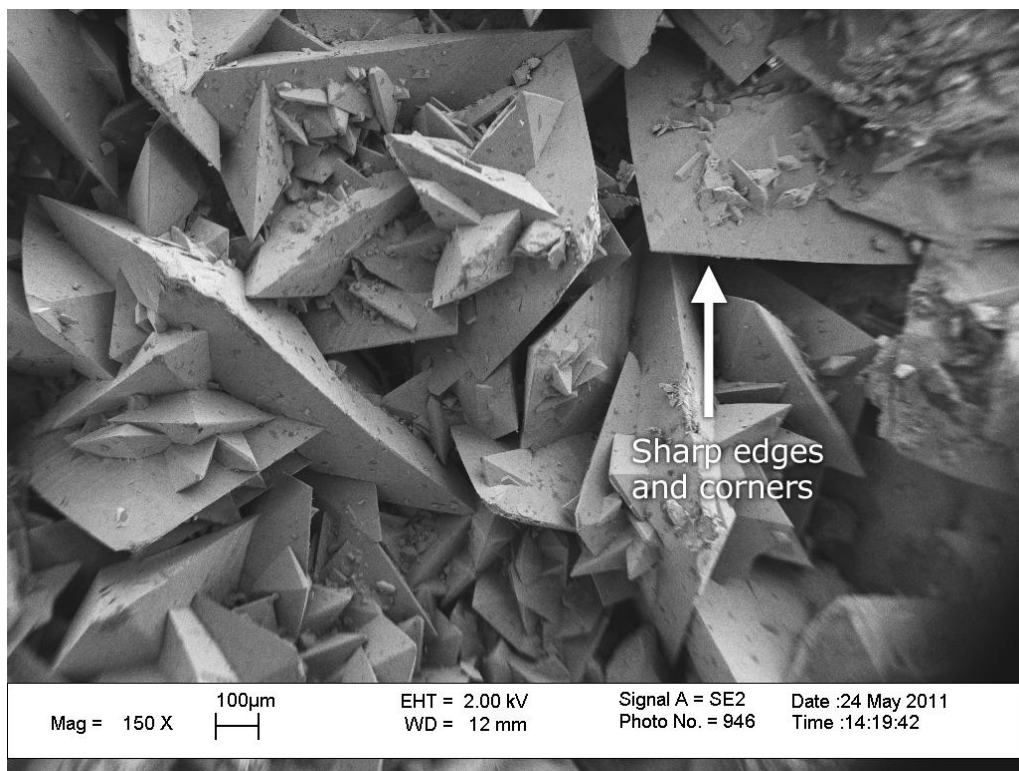
4.1 Conclusion of Hydrodynamic Cavitation Study

4.1.1 Conclusion of Hydrodynamic Cavitation Application to Chalk and Cancerous Cells

The treatment duration for lithotripsy typically varies from 5-160 min and has an average of 30 minutes for the most treatment sessions. For the alternative technique of hydrodynamic cavitation considered in this study, above mentioned kidney stones were broken into pieces with a short time of 25-30 minutes, which has a significant overlap in the duration with the lithotripsy method. By optimizing the experimental conditions such as microprobe geometry, microprobe size, the distance between the kidney stone and microprobe and the use of multiple microprobes, significant improvement of the performance of the proposed technique could be attained. These promising results suggest that hydrodynamic cavitation in micro scale has a potential of being a strong alternative for ultrasound therapy. Ultrasound therapy offers the remote application advantage. However, using micro manipulator could provide fine control of the exposure of bubbly hydrodynamic cavitation on the target area so that localized therapy could be expected. Concentrated efforts and future work on this area should yield a prototype that could have a highly targeted, localized, and controlled effect on kidney stones, so that other areas in the vicinity will not be affected unwanted effects to the surrounding normal tissue will be minimized. This prototype could provide a cost effective and energy efficient solution for kidney stone therapy. It is expected that the prototype would have a manufacturing cost lower than \$10,000. Taking administrative and marketing expenses into consideration, the unit price of the hydrodynamic cavitation device is expected to be in the competitive range with commercially available products based on lithotripsy [69].

Surface characteristics of the tested kidney stone samples are carefully investigated by SEM technique (Scanning Electron Microscope) and a high resolution light microscope. Surface morphology before and after hydrodynamic cavitation exposure of the tested kidney stones are compared based on SEM images (Figure 22). A significant

difference in the stones' surface has been observed in the form of a change in surface roughness compared to the unexposed surfaces. Accordingly, crystal-like surface structure of the kidney stone samples was "shaved off" after the micro-mechanical erosion generated by cavitating bubbly flows during the experiments. As can be observed, sharpness of the edges and corners are significantly reduced after the cavitation exposure. After each experiment, stone debris was analyzed under a light microscope. Maximum debris size is found to be around 110 μm . (Figure 12) Small debris size implies that there will be no difficulties for the debris to pass through the urinary tract.



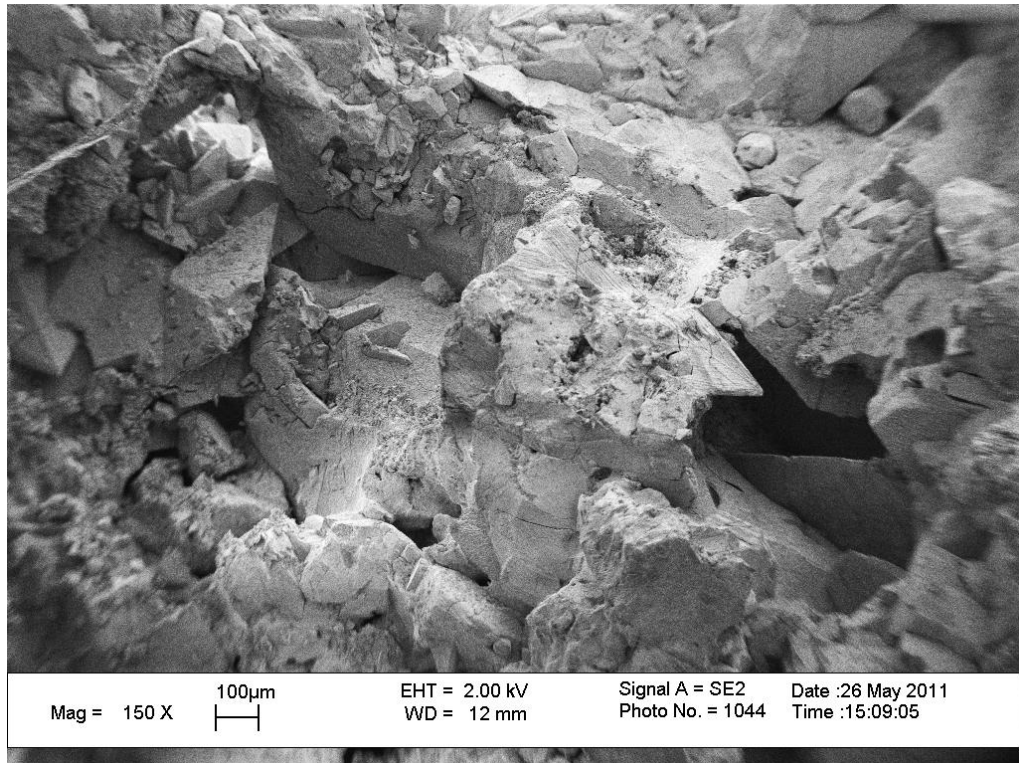


Figure 22 Calcium oxalate kidney stone (a) before hydrodynamic cavitation exposure, (b) after hydrodynamic cavitation exposure.

The results from the experiments have shown that hydrodynamic cavitation could be used as a promising alternative to ultrasound therapy methods for kidney stone treatment. Micro scale hydrodynamic cavitation offers several advantages such as fine controllability, low power consumption, low heat generation, and successful targeting. It is more energy efficient and cost effective compared to the other methods, whereas the therapy duration also well overlaps with the therapy duration ranges for the other methods. Indeed, the diameter of the cavitation probe and the tubing is 1.56 mm, a size that can fit in a regular 5 mm endoscopy device. (Figure 23, Figure 24)

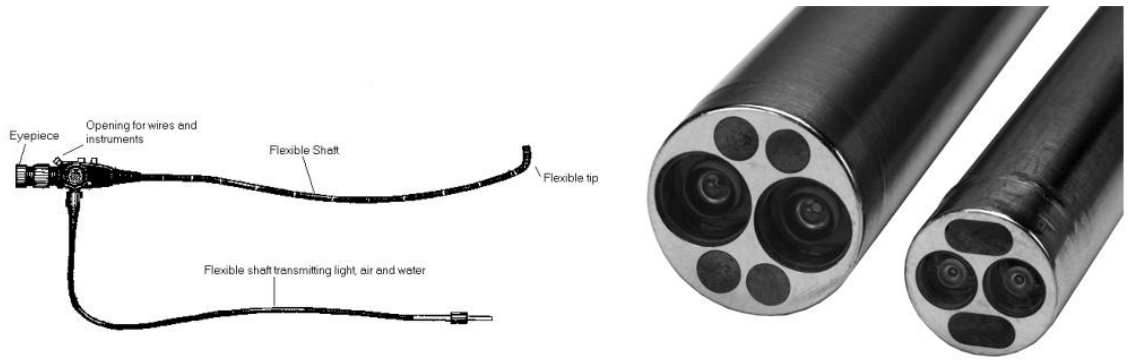


Figure 23 A typical endoscopy device

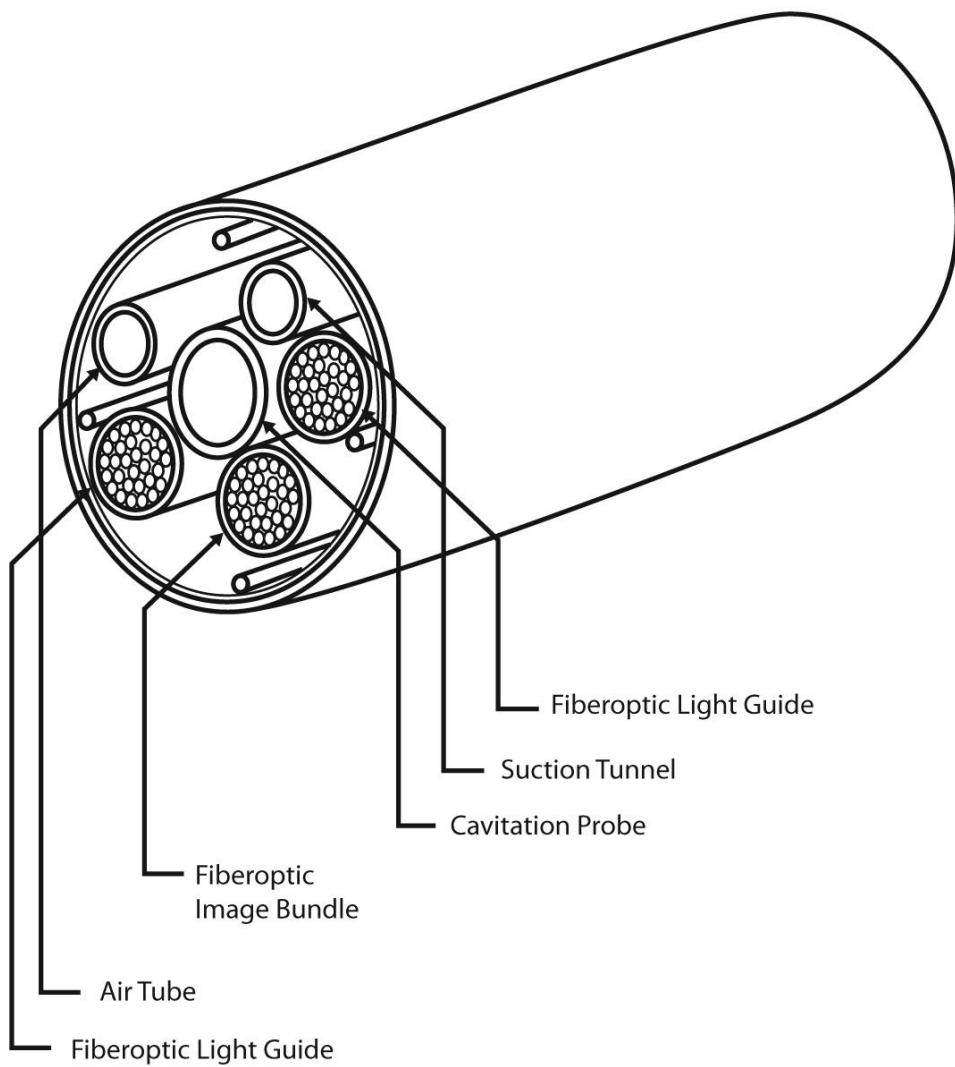


Figure 24 Crosssection of cavitation probe integration for endoscope

Its destructive effects were proven on kidney stones in this study. The liquid (Phosphate buffered saline) used in the experiments is non-toxic and isotonic to the human body. Moreover, the liquid planned to be discharged from the body simultaneously during the application using a parallel discharge line. Therefore, we believe the method is a practical option to used in human body. However, further *in vivo* animal studies and clinical studies are needed for better understanding and characterization of the possible outcomes of the proposed method.

4.1.2 Conclusion of Hydrodynamic Cavitation Application to Prostate Cells and Tissue

Hydrodynamic cavitation was targeted to prostate cancer cells; PC-3 and DU-145 under an inlet pressure of 150 PSI for 1, 2, 3 and 5 minutes. Control samples were unexposed to cavitation. Hydrodynamic cavitation caused a dramatic decrease in cell number in a exposure time dependent manner.

Hydrodynamic cavitation effect on prostate cancer cells; PC-3 and DU-145 A) with a pressure kinetics (50, 100 and 150 PSI) at a constant exposure time (5 min) was checked by means of apoptotic activity at 0 h (immediately after cavitation) and 24 hours after cavitation. Control samples were unexposed to cavitation. 8 μ M Staurosporine and 10 μ M Cisplatin treated samples are used as positive control for apoptosis activation. Apoptotic activity was not induced following to hydrodynamic cavitation exposure on prostate cells. No PARP cleavage and caspases activation was checked after cavitation.

PC-3 cells were exposed to 150 PSI, 5 min cavitation and cultured for 0, 6, 12 and 24 hours. Control samples were unexposed to cavitation. There was no difference in cell cycle of cavitation exposed cells in comparison to cavitation unexposed cells. Cell cycle arrest analysis of PC-3 was performed by flow cytometry at 0, 6, 12 and 24 hours after cavitation. The reduction of cell growth following to hydrodynamic cavitation was not caused by neither cell cycle arrest nor DNA fragmentation.

Cavitation control (at same flow rate, yet different pressure with cavitation) and cavitation (1450 PSI) was applied to BPH tissues for 15 and 30 minutes, and the resulting changes were observed under 40X. Hydrodynamic cavitation could successfully erode human BPH tissues effectively and precisely.

References

- [1] C. T. Crowe, *Multiphase Flow Handbook*. Boca Raton, FL: CRC, 2006.
- [2] <http://www.hydro-tg.fr/>. (2012) <http://hydro.tg.free.fr/>. [Online]. http://hydro.tg.free.fr/reparation_pompe/cavitation/cavitation.jpg
- [3] A B Pandit V S Moholkar, "Modeling of hydrodynamic cavitation reactors: a unified approach," *Chemical Engineering Science*, vol. 56, pp. 6295-6302, 2001.
- [4] A B Pandit V S Moholkar, "Numerical investigations in the behavior of one-dimensional bubbly flow in hydrodynamic cavitation," *Chemical Engineering Science*, vol. 56, pp. 1411-1418, 2001.
- [5] Y. Benito S. Arrojo, "A theoretical study of hydrodynamic cavitation," *Ultrasonics Sonochemistry*, vol. 15, pp. 203-211, 2008.
- [6] Y Peles C Mishra, "Flow visualization of cavitating flows through a rectangular slot micro-orifice ingrained in a microchannel," *Phys. Fluids*, vol. 17, pp. 113602-113615, 2005.
- [7] Y Peles C Mishra, "Size scale effects on cavitating flows through microorifices entrenched in rectangular microchannels," *Journal of Microelectromechanical Systems*, vol. 14, pp. 987-999, 2005.
- [8] Y Peles C Mishra, "An experimental investigation of hydrodynamic cavitation in micro-venturis," *Phys. Fluids*, vol. 18, pp. 103603-103607, 2006.
- [9] Y Peles C Mishra, "Cavitation in flow through a micro-orifice inside a silicon microchannel," *Phys. Fluids*, vol. 17, pp. 013601-013615, 2005.
- [10] A Koşar, C J Kuo, C Mishra, G S Cole, R P Scaringe, Y Peles B Schneider, "Cavitation enhanced heat transfer in microchannels," *Journal of Heat Transfer*, vol. 128, pp. 1293-1301, 2006.
- [11] C E Brennen, *Cavitation and Bubble Dynamics*. London, U.K.: Oxford Univ. Press, 1995.
- [12] A Shima Y Tomita, "Mechanisms of impulsive pressure generation and damage pit formation by bubble collapse," *Journal of Fluid Mechanics*, vol. 169, pp. 535-564, 1986.
- [13] Phillip Eisenberg, "Cavitation Damage," Washington, D.C., 1963.
- [14] C. E. Brennen, *Fundamentals of Multiphase Flow*. New York: Cambridge Univ. Press, 2005.
- [15] Achiau Ludomirsky, Lucy Eun, Timothy Hall, Binh Tran, Brian Fowlkes, Charles Cain Zhen Xu, "Controlled Ultrasound Tissue Erosion," *IEEE Trans Ultrason Ferroelectr Freq Control*, vol. 51, no. 6, pp. 726-736, 2004.
- [16] E Chen ,C Lee LA Frizzell, "Effects of pulsed ultrasound on the mouse neonate: hind limb paralysis and lung hemorrhage," *Ultrasound in Medicine & Biology*, vol. 20, no. 1, pp. 53-63, 1994.
- [17] CH Raeman,SZ Child, EL Carstensen EL D Dalecki, "Intestinal hemorrhage from exposure to pulsed ultrasound," *Ultrasound Med Biol*, vol. 21, pp. 1067-1072, 1995.
- [18] Y Peles C Mishra, "Flow visualization of cavitating flows through a rectangular slot micro-orifice ingrained in a microchannel," *Phys. Fluids*, vol.

- 17, pp. 113602-113615, 2005.
- [19] Y Peles C Mishra, "Size scale effects on cavitating flows through microorifices entrenched in rectangular microchannels," *Journal of Microelectromechanical Systems*, vol. 14, pp. 987-999, 2005.
- [20] Y Peles C Mishra, "An experimental investigation of hydrodynamic cavitation in micro-venturis," *Phys. Fluids*, vol. 18, pp. 103603-103607, 2006.
- [21] Y Peles C Mishra, "Cavitation in flow through a micro-orifice inside a silicon microchannel," *Phys Fluids*, vol. 17, pp. 013601-013615, 2005.
- [22] A Koşar, C J Kuo, C Mishra, G S Cole, R P Scaringe, Y Peles B Schneider, "Cavitation enhanced heat transfer in microchannels," *Journal of Heat Transfer*, vol. 128, pp. 1293-1301, 2006.
- [23] A. P. Evan and J. A. McAteer,. Philadelphia, PA: Lippincott-Raven, 1996, pp. 549-570.
- [24] J. A. McAteer and A. P. Evan, "The Acute and Long-Term Adverse Effects of Shock Wave Lithotripsy," *Semin. Nephrol*, vol. 28, pp. 200-213, 2008.
- [25] McAteer J. A. Evan A. P., *Q-effects of shock wave lithotripsy*. Philadelphia: American Urological Association Education and Research, Inc., 1996.
- [26] A Evan, E Worcester F L Coe, "Kidney Stone Disease," *The Journal of Clinical Investigation*, vol. 115, pp. 2598-2608, 2005.
- [27] A. Kosar, M. Sesen, Z. Itah, O. Oral, and D. Gozuacik, "Bubbly Cavitating Flow Generation and Investigation of Its Erosional Nature for Biomedical Applications," *IEEE Transactions on Biomedical Engineering*, vol. 58, no. 5, pp. 1337-1346, 2011.
- [28] Rooney JA, "Hydrodynamic shearing of biological cells," *Biol Phys*, vol. 2, pp. 26-40, 1973.
- [29] Rooney JA, "Shear as a mechanism for sonically induced biological effects.," *J Acoust Soc Am*, vol. 52, no. 6, pp. 1718-1724, 1972.
- [30] and Mason TJ Povey MJW, *Ultrasound in food processing*. New York: Blackie Academic & Professional, 1998.
- [31] AJ Carmichael, MM Mossoba, P Riesz GL Christman, "Evidence for free radicals produced in aqueous solutions by diagnostic ultrasound," *Ultrasonics*, vol. 25, no. 1, pp. 31-34, 1987.
- [32] Leon A. Rozenszajn, Michal Blass, Mira Barda-Saad, Damir Azimov, Judith Radnay, Dov Zipori and Uri Rosenschein Hagit Ashush, "Apoptosis induction of human myeloid leukemic cells by ultrasound exposure," *Cancer Research*, vol. 60, no. 4, pp. 1014-1020, 2000.
- [33] de Meulenaer EC, Delforge A, Dejeneffe M, Massy M, Moerman C, Hannecart B, Canivet Y, Lepeltier MF, and Bron D. Lagneaux L, "Ultrasonic low-energy treatment: a novel approach to induce apoptosis in human leukemic cells," *Exp Hematol*, vol. 30, no. 11, pp. 1293-1301, 2002.
- [34] Jr., Kondo T, Cui ZG, Tabuchi Y, Zhao QL, Ando H, Misaki T, Yoshikawa H, and Umemura S. Feril LB, "Apoptosis induced by the sonomechanical effects of low intensity pulsed ultrasound in a human leukemia cell line," *Cancer Lett* , vol. 221, no. 2, pp. 145-152, 2005.

- [35] Andoc H, Takasakia I, Feril LB, Zhaob QL, Ogawab R, Kudod N, Tachibanae K, Kondob T, Tabuchia Y, "Identification of genes responsive to low intensity pulsed ultrasound in a human leukemia cell line Molt-4," *Cancer Letters*, vol. 246, no. 1-2, pp. 149–156, 2007.
- [36] Kondo T, Zhao Q.L., Feril Jr L.B., Kitagawa H, Honda H, "Role of intracellular calcium ions and reactive oxygen species in apoptosis induced by ultrasound," *Ultrasound Med. Biol.*, vol. 30, pp. 683–692, 2004.
- [37] S Harrison B Balasundaram, "Disruption of Brewers' yeast by hydrodynamic cavitation: Process variables and their influence on selective release," *Biotechnol Bioeng*, vol. 94, no. 2, pp. 303-311, 2006.
- [38] ST Harrison B Balasundaram, "Study of physical and biological factors involved in the disruption of E. coli by hydrodynamic cavitation," *Biotechnol Prog*, vol. 22, no. 3, pp. 907-913, 2006.
- [39] Wang J, Guo P, Guo W, and Wang C. Wang X, "Degradation of rhodamine B in aqueous solution by using swirling jet-induced cavitation combined with H₂O₂," *J Hazard Mater*, vol. 169, no. 1-3, pp. 486-491, 2009.
- [40] Braeutigam P, Wu ZL, Ren Y, and Ondruschka B. Franke M, "Enhancement of chloroform degradation by the combination of hydrodynamic and acoustic cavitation," *Ultrason Sonochem*, vol. 18, no. 4, pp. 888-894, 2011.
- [41] Toledo RT, Chen J, and Kazem B. Milly PJ, "Hydrodynamic cavitation to improve bulk fluid to surface mass transfer in a nonimmersed ultraviolet system for minimal processing of opaque and transparent fluid foods," *J Food Sci*, vol. 72, no. 9, pp. 407-413, 2007.
- [42] Toledo RT, Harrison MA, and Armstead D. Milly PJ, "Inactivation of food spoilage microorganisms by hydrodynamic cavitation to achieve pasteurization and sterilization of fluid foods," *J Food Sci*, vol. 72, no. 9, pp. 414-422, 2007.
- [43] Wang J., Li Y., Yu Y., Xu Z. Ji J., "Preparation of biodiesel with the help of ultrasonic and hydrodynamic cavitation," *Ultrasonics*, vol. 44, pp. e411–e414, 2006.
- [44] Moser WR, and Guerts BM. Sunstrom IE, "General route to nanocrystalline oxides by hydrodynamic cavitation," *Chem. Mater.*, vol. 8, pp. 2061–2067, 1996.
- [45] Nguyen DX, Khan S, Prausnitz MR. Guzmán HR, "Ultrasound-mediated disruption of cell membranes. I. Quantification of molecular uptake and cell viability," *J Acoust Soc Am.*, vol. 110, no. 1, pp. 588-96, 2001.
- [46] L. B. Feril Jr. et al., "Apoptosis Induced by the Sonomechanical Effects of Low Intensity Pulsed Ultrasound in a Human Leukemia Cell Line," *Cancer Lett.*, vol. 221, pp. 145-152, 2005.
- [47] McDannold N, Martin H, Bronson RT, and Hynynen K. Vykhodtseva N, "Apoptosis in ultrasound-produced threshold lesions in the rabbit brain," *Ultrasound Med Biol*, vol. 27, no. 1, pp. 111-117, 2001.
- [48] Prat F, Chapelon JY, Abou el Fadil F, Henry L, Theillere Y, Ponchon T, and Cathignol D. Sibille A, "Extracorporeal ablation of liver tissue by high-intensity focused ultrasound," *Oncology*, vol. 50, no. 5, pp. 375-379, 1993.

- [49] J Margonari, F Vernier, F Gorry, R Ecochard, A Gelet JY Chapelon, "In vivo effects of high-intensity ultrasound on prostatic adenocarcinoma Dunning R3327.," *Cancer Res*, vol. 52, no. 22, pp. 6353-6357, 1992.
- [50] Muramoto M, Kyunou H, Iwamura M, Egawa S, Koshiba K, Uchida T, "Clinical outcome of high-intensity focused ultrasound for treating benign prostatic hyperplasia: preliminary report," *Urology*, vol. 52, pp. 66-71, 1998.
- [51] Pedevilla M, Vingers L, Susani M, Marberger M, Madersbacher S, "Effect of high-intensity focused ultrasound on human prostate cancer in vivo.," *Cancer Res*, vol. 55, pp. 3346-3351, 1995.
- [52] Wang ZB, Cao Y-De, Chen WZ, Bai J, Zou JZ, Zhu H, Wu F, "A randomised clinical trial of high-intensity focused ultrasound ablation for the treatment of patients with localised breast cancer.," *British Journal of Cancer*, vol. 89, pp. 2227 – 2236, 2003.
- [53] Wang Z, Chen W, Wu F, "Pathological study of extracorporeally ablated hepatocellular carcinoma with high-intensity focused ultrasound," *Zhonghua Zhong Liu Za Zhi*, vol. 23, pp. 237-239, 2001.
- [54] Song J, Miller DL, "Tumor growth reduction and DNA transfer by cavitation-enhanced high-intensity focused ultrasound in vivo," *Ultrasound in Medicine & Biology*, vol. 29, no. 6, pp. 887–893, 2003.
- [55] Wang ZB, Zhu H, Chen WZ, Zou JZ, Bai J, Li KQ, Jin CB, Xie FL, Su HB, Wu F, "US-guided high-intensity focused ultrasound treatment in patients with advanced pancreatic cancer: Initial experience," *Radiology*, vol. 236, pp. 1034-1040, 2005.
- [56] CH Farny, GT Haar, RA Roy CC Coussios, "Role of acoustic cavitation in the delivery and monitoring of cancer treatment by high-intensity focused ultrasound (HIFU).," *Int J Hyperthermia*, vol. 23, no. 2, pp. 105-120, 2007.
- [57] Yu-Feng Zhou, "High intensity focused ultrasound in clinical tumor ablation.," *World J Clin Oncol*, vol. 2, no. 1, pp. 8-27, 2011.
- [58] Wang ZB, Cao YD, Xu ZL, Zhou Q, Zhu H, Chen WZ, Wu F, "Heat fixation of cancer cells ablated with high-intensity-focused ultrasound in patients with breast cancer.," *American J Surgery*, vol. 192, no. 2, pp. 179-84, 2006.
- [59] S Rogenhofer, R Ganzer, PJ Wild, WF Wieland, B Walter A Blana, "Morbidity associated with repeated transrectal high-intensity focused ultrasound treatment of localized prostate cancer," *World J Urol*, vol. 24, pp. 585-590, 2006.
- [60] Ki-Jun Lee, and Yongsok Seo Sehyun Kim, "Polyetheretherketone (PEEK) surface functionalization by low-energy ion-beam irradiation under a reactive O₂ environment and Its effect on the PEEK/Copper adhesives," *Langmuir*, vol. 20, no. 1, pp. 157-163, 2004.
- [61] D. Heimbach et al., "Acoustic and Mechanical Properties of Artificial Stones in comparison to Natural Kidney Stones," *J. Urol.*, vol. 164, pp. 537-544, 2000.
- [62] Xie Chong, "Subsonic choked flow in the microchannel," *Physics of Fluids*, no. 18, 2006.
- [63] C. Mishra and Y. Peles, "Flow Visualization of Cavitating Flows through a Rectangular Slot micro-orifice Ingrained in a microchannel," *Phys. Fluids*,

vol. 17, pp. 113602-113615, 2005.

- [64] Finnie L. Sheldon G. L., "The mechanism of material removal in the erosive cutting of brittle materials," *ASME Journal of Engineering in Industry*, vol. 88B, pp. 393-400, 1966.
- [65] Daniel J Klionsky Beth Levine, "Development by Self-Digestion: Molecular Mechanisms and Biological Functions of Autophagy," *Developmental Cell*, vol. 6, no. 4, pp. 463-477, 2004.
- [66] C. Goldenstedt et al., "Cavitation Enhances Treatment Depth When Combined with Thermal Effect using a Plane Ultrasound Transducer: An in vivo study," *Proc. IEEE Ultrason. Symp.*, vol. 1, pp. 709-712, 2004.
- [67] D. Gozuacik and A. Kimchi, "Autophagy and Cell Death," *Curr. Topics Dev. Biol.*, vol. 78, pp. 217-245, 2007.
- [68] D. Gozuacik et al., "DAP-kinase is a Mediator of Endoplasmic Reticulum Stress-Induced Caspase Activation and Autophagic Cell Death," *Cell Death Differ.*, vol. 15, pp. 1875-1886, 2008.
- [69] R Chuttani, J Croffie J DiSario, "Flow visualization of cavitating flows through a rectangular slot micro-orifice ingrained in a microchannel," *Gastrointestinal Endoscopy*, vol. 65, pp. 750-756, 2007.
- [70] A. Kosar et al., "Bubbly Cavitating Flow Generation and Investigation of Its Erosional Nature for Biomedical Applications," in *Proceedings of 2nd Micro and Nano Flows Conference*, West London, UK., 2009.
- [71] C. Mishra and Y. Peles, "Size Scale Effects on Cavitating Flows through microorifices Entrenched in Rectangular microchannels," *J. Microelectromech. Syst.*, vol. 14, pp. 987-999, 2005.
- [72] C. Mishra and Y. Peles, "An Experimental Investigation of Hydrodynamic Cavitation in micro-venturis," *Phys. Fluids*, vol. 18, pp. 103603-103607, 2006.
- [73] C. Mishra and Y. Peles, "Cavitation in Flow through a micro-orifice inside a Silicon microchannel," *Phys. Fluids*, vol. 17, pp. 013601-013615, 2005.